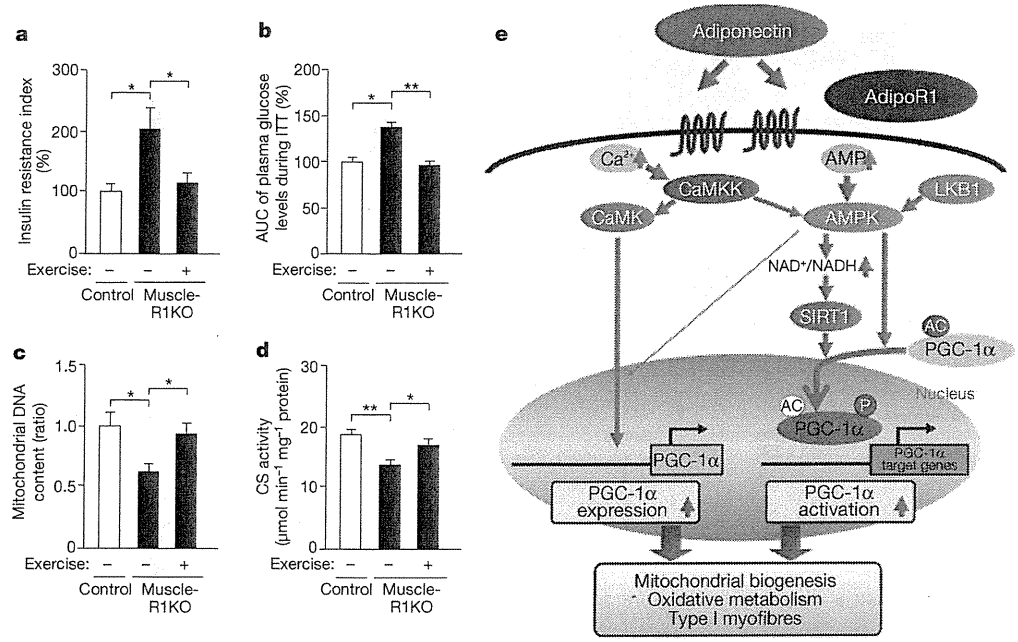


**Figure 6 | The effect of exercise on muscle-R1KO mice. a–d,** The insulin resistance index (**a**), area under the curves (AUC) of plasma glucose levels during the ITT (**b**), mitochondrial content as assessed by mitochondrial DNA copy number (**c**), and citrate synthase (CS) enzyme activity (**d**) in skeletal muscle of control and muscle-R1KO mice after 2 weeks exercise. The results are expressed as the percentage of the value in control littermates (**a, b**). **e,** Scheme illustrating the signal transduction of adiponectin/AdipoR1 in muscle cells. Both CaMKKβ and LKB1 are necessary for adiponectin-induced full AMPK activation. AMPK and SIRT1 are required for adiponectin/AdipoR1-induced PGC-1α activation. CaMKKβ activation by adiponectin-induced $Ca^{2+}$ influx via AdipoR1 is required for adiponectin-induced increased PGC-1α expression. PGC-1α is required for mitochondrial biogenesis stimulated with adiponectin/AdipoR1. From these data, we conclude that adiponectin and AdipoR1 increase PGC-1α expression and activity by $Ca^{2+}$ signalling and by AMPK and SIRT1, leading to increased mitochondrial biogenesis. We focused on the molecules that we have obtained direct evidence by both gain-of-function and loss-of-function experiments *in vitro* and *in vivo*, except for CaMK, which has already been reported to increase PGC-1α expression by other researchers[39]. AC, acetylation. All values are presented as mean ± s.e.m. $n = 5–8$, $^{*}P < 0.05$ and $^{**}P < 0.01$ compared to control mice or as indicated.

adiponectin/AdipoR1 in pathophysiological conditions such as obesity may have causal roles in the development of PGC-1α dysregulation and mitochondrial dysfunction.

In skeletal muscle AdipoR1 regulated insulin sensitivity by several mechanisms (Supplementary Fig. 7). First is the activation of S6K1, which has been reported to be able to cause insulin resistance by increased phosphorylation of Ser 636/639 in IRS-1 (ref. 27). S6K1 is crucially inhibited by AMPK[43]. In skeletal muscle of muscle-R1KO mice, AMPK activation was reduced, whereas activation of S6K1 and phosphorylation of Ser 636/639 in IRS-1 were indeed increased. Second is the increased oxidative stress, which has been causally linked to insulin resistance[44] by increased phosphorylation of Ser 302 in IRS-1 through JNK activation[26]. Several oxidative stress detoxification genes are crucially regulated by AMPK and PGC-1α[45], and the expression levels of these genes such as *Sod2* and *Cat* were reduced, which was associated with increased TBARS in skeletal muscle of muscle-R1KO mice. Third is the increased triglyceride content, which has been associated with insulin resistance by increased phosphorylation of Ser 302 in IRS-1 through JNK activation[26]. Molecules involved in fatty-acid oxidation are crucially regulated by AMPK and PGC-1α, and the expression levels of these genes such as *Mcad* were reduced, which was associated with increased triglyceride content in skeletal muscle of muscle-R1KO mice. Consistent with increased TBARS and triglyceride content, JNK activation and phosphorylation of Ser 302 in IRS-1 were indeed increased.

Exercise has been reported to have beneficial effects on longevity and lifestyle-related diseases, and at the same time to activate $Ca^{2+}$, AMPK, SIRT1 and PGC-1α pathways[39]. In this study, we clearly demonstrated that adiponectin and AdipoR1 regulate PGC-1α and mitochondria via $Ca^{2+}$ and AMPK/SIRT1. Therefore, agonism of AdipoR1 as well as strategies to increase AdipoR1 in muscle could be exercise-mimetics.

In conclusion, AdipoR1 has a crucial role in the physiological and pathophysiological significance of adiponectin in muscle, and is involved in the regulation of $Ca^{2+}$ signalling, PGC-1α expression and activation, mitochondrial function and oxidative stress, glucose and lipid metabolism, and exercise endurance. This study suggests that agonism of AdipoR1, as well as strategies to increase AdipoR1 in muscle, may be logical approaches to providing a new treatment modality for mitochondrial dysfunction, insulin resistance and type 2 diabetes linked to obesity.

## METHODS SUMMARY

**Mice.** Mice were 8–10 weeks of age at the time of the experiment. The animal care and use procedures were approved by the Animal Care Committee of the University of Tokyo.

**Measurement of exercise capacity in muscle-R1KO mice.** The treadmill exercise test regimen was 15 m $min^{-1}$ for 20 min. Exercise endurance was assessed by dividing 20 min by the number of times a mouse was unable to avoid electrical shocks.

**Studies with C2C12 cells.** Induction of myogenic differentiation was carried out according to a method described previously[11]. By day 5, the cells had differentiated into multinucleated contracting myocytes. C2C12 myocytes were used after myogenic differentiation in all experiments.

**Plasmids.** The plasmids encoding PGC-1α and the PGC-1α-2A mutant were generous gifts from B. M. Spiegelman, and have all been described previously[31]. The plasmids encoding for the PGC-1α-R13 mutant were generous gifts from P. Puigserver, and have all been described previously[32].

**Statistical analysis.** Results are expressed as mean ± s.e.m. Differences between two groups were assessed using unpaired two-tailed *t*-tests. Data involving more than two groups were assessed by analysis of variance (ANOVA).

**Received 12 August 2009; accepted 11 March 2010.**
**Published online 31 March 2010.**

1. Scherer, P. E., Williams, S., Fogliano, M., Baldini, G. & Lodish, H. F. A novel serum protein similar to C1q, produced exclusively in adipocytes. *J. Biol. Chem.* 270, 26746–26749 (1995).

2. Hu, E., Liang, P. & Spiegelman, B. M. AdipoQ is a novel adipose-specific gene dysregulated in obesity. *J. Biol. Chem.* **271**, 10697–10703 (1996).
3. Maeda, K. *et al.* cDNA cloning and expression of a novel adipose specific collagen-like factor, apM1 (AdiPose Most abundant Gene transcript 1). *Biochem. Biophys. Res. Commun.* **221**, 286–289 (1996).
4. Nakano, Y., Tobe, T., Choi-Miura, N.-H., Mazda, T. & Tomita, M. Isolation and characterization of GBP28, a novel gelatin-binding protein purified from human plasma. *J. Biochem.* **120**, 803–812 (1996).
5. Hotta, K. *et al.* Plasma concentrations of a novel, adipose-specific protein, adiponectin, in type 2 diabetic patients. *Arterioscler. Thromb. Vasc. Biol.* **20**, 1595–1599 (2000).
6. Fruebis, J. *et al.* Proteolytic cleavage product of 30-kDa adipocyte complement-related protein increases fatty acid oxidation in muscle and causes weight loss in mice. *Proc. Natl Acad. Sci. USA* **98**, 2005–2010 (2001).
7. Yamauchi, T. *et al.* The fat-derived hormone adiponectin reverses insulin resistance associated with both lipoatrophy and obesity. *Nature Med.* **7**, 941–946 (2001).
8. Berg, A. H., Combs, T. P., Du, X., Brownlee, M. & Scherer, P. E. The adipocyte-secreted protein Acrp30 enhances hepatic insulin action. *Nature Med.* **7**, 947–953 (2001).
9. Kubota, N. *et al.* Disruption of adiponectin causes insulin resistance and neointimal formation. *J. Biol. Chem.* **277**, 25863–25866 (2002).
10. Maeda, N. *et al.* Diet-induced insulin resistance in mice lacking adiponectin/ACRP30. *Nature Med.* **8**, 731–737 (2002).
11. Yamauchi, T. *et al.* Adiponectin stimulates glucose utilization and fatty-acid oxidation by activating AMP-activated protein kinase. *Nature Med.* **8**, 1288–1295 (2002).
12. Tomas, E. *et al.* Enhanced muscle fat oxidation and glucose transport by ACRP30 globular domain: acetyl-CoA carboxylase inhibition and AMP-activated protein kinase activation. *Proc. Natl Acad. Sci. USA* **99**, 16309–16313 (2002).
13. Kahn, B. B., Alquier, T., Carling, D. & Hardie, D. G. AMP-activated protein kinase: ancient energy gauge provides clues to modern understanding of metabolism. *Cell Metab.* **1**, 15–25 (2005).
14. Kersten, S., Desvergne, B. & Wahli, W. Roles of PPARs in health and disease. *Nature* **405**, 421–424 (2000).
15. Yamauchi, T. *et al.* Globular adiponectin protected ob/ob mice from diabetes and apoE deficient mice from atherosclerosis. *J. Biol. Chem.* **278**, 2461–2468 (2003).
16. Yamauchi, T. *et al.* Cloning of adiponectin receptors that mediate antidiabetic metabolic effects. *Nature* **423**, 762–769 (2003).
17. Wess, J. G-protein-coupled receptors: molecular mechanisms involved in receptor activation and selectivity of G-protein recognition. *FASEB J.* **11**, 346–354 (1997).
18. Yokomizo, T., Izumi, T., Chang, K., Takuwa, Y. & Shimizu, T. A. G-protein-coupled receptor for leukotriene B4 that mediates chemotaxis. *Nature* **387**, 620–624 (1997).
19. Scheer, A., Fanelli, F., Costa, T., De Benedetti, P. G. & Cotecchia, S. Constitutively active mutants of the α1B-adrenergic receptor: role of highly conserved polar amino acids in receptor activation. *EMBO J.* **15**, 3566–3578 (1996).
20. Yamauchi, T. *et al.* Targeted disruption of AdipoR1 and AdipoR2 causes abrogation of adiponectin binding and metabolic actions. *Nature Med.* **13**, 332–339 (2007).
21. Petersen, K. F. *et al.* Impaired mitochondrial activity in the insulin-resistant offspring of patients with type 2 diabetes. *N. Engl. J. Med.* **350**, 664–671 (2004).
22. Wu, Z. *et al.* Mechanisms controlling mitochondrial biogenesis and respiration through the thermogenic coactivator PGC-1. *Cell* **98**, 115–124 (1999).
23. Mootha, V. K. *et al.* Errα and Gabpa/b specify PGC-1α-dependent oxidative phosphorylation gene expression that is altered in diabetic muscle. *Proc. Natl Acad. Sci. USA* **101**, 6570–6575 (2004).
24. Berchtold, M. W. *et al.* Calcium ion in skeletal muscle: its crucial role for muscle function, plasticity, and disease. *Physiol. Rev.* **80**, 1215–1265 (2000).
25. Wu, H. *et al.* MEF2 responds to multiple calcium-regulated signals in the control of skeletal muscle fiber type. *EMBO J.* **19**, 1963–1973 (2000).
26. Hotamisligil, G. S. Inflammation and metabolic disorders. *Nature* **444**, 860–867 (2006).
27. Um, S. H. *et al.* Absence of S6K1 protects against age- and diet-induced obesity while enhancing insulin sensitivity. *Nature* **431**, 200–205 (2004).
28. Hawley, S. A. *et al.* Characterization of the AMP-activated protein kinase kinase from rat liver and identification of threonine 172 as the major site at which it phosphorylates AMP-activated protein kinase. *J. Biol. Chem.* **271**, 27879–27887 (1996).
29. Hawley, S. A. *et al.* Calmodulin-dependent protein kinase kinase-β is an alternative upstream kinase for AMP-activated protein kinase. *Cell Metab.* **2**, 9–19 (2005).
30. Woods, A. *et al.* $Ca^{2+}$/calmodulin-dependent protein kinase kinase-β acts upstream of AMP-activated protein kinase in mammalian cells. *Cell Metab.* **2**, 21–33 (2005).
31. Jäger, S., Handschin, C., St-Pierre, J. & Spiegelman, B. M. AMP-activated protein kinase (AMPK) action in skeletal muscle via direct phosphorylation of PGC-1α. *Proc. Natl Acad. Sci. USA* **104**, 12017–12022 (2007).
32. Rodgers, J. T. *et al.* Nutrient control of glucose homeostasis through a complex of PGC-1α and SIRT1. *Nature* **434**, 113–118 (2005).
33. Guarente, L. Sirtuins as potential targets for metabolic syndrome. *Nature* **444**, 868–874 (2006).
34. Tokumitsu, H. *et al.* STO-609, a specific inhibitor of the $Ca^{2+}$/calmodulin-dependent protein kinase kinase. *J. Biol. Chem.* **277**, 15813–15818 (2002).
35. Tóth, A. *et al.* Quantitative assessment of $[Ca^{2+}]_i$ levels in rat skeletal muscle *in vivo*. *Am. J. Physiol. Heart Circ. Physiol.* **275**, H1652–H1662 (1998).
36. Shkryl, V. M. & Shirokova, N. Transfer and tunneling of $Ca^{2+}$ from sarcoplasmic reticulum to mitochondria in skeletal muscle. *J. Biol. Chem.* **281**, 1547–1554 (2006).
37. Anderson, K. A. *et al.* Components of a calmodulin-dependent protein kinase cascade. Molecular cloning, functional characterization and cellular localization of $Ca^{2+}$/calmodulin-dependent protein kinase kinase beta. *J. Biol. Chem.* **273**, 31880–31889 (1998).
38. Soderling, T. R. The Ca-calmodulin-dependent protein kinase cascade. *Trends Biochem. Sci.* **24**, 232–236 (1999).
39. Handschin, C. & Spiegelman, B. M. The role of exercise and PGC1α in inflammation and chronic disease. *Nature* **454**, 463–469 (2008).
40. Handschin, C. *et al.* Skeletal muscle fiber-type switching, exercise intolerance, and myopathy in PGC-1α muscle-specific knock-out animals. *J. Biol. Chem.* **282**, 30014–30021 (2007).
41. Mootha, V. K. *et al.* PGC-1α-responsive genes involved in oxidative phosphorylation are coordinately downregulated in human diabetes. *Nature Genet.* **34**, 267–273 (2003).
42. Patti, M. E. *et al.* Coordinated reduction of genes of oxidative metabolism in humans with insulin resistance and diabetes: Potential role of PGC1 and NRF1. *Proc. Natl Acad. Sci. USA* **100**, 8466–8471 (2003).
43. Wang, C. *et al.* Adiponectin sensitizes insulin signaling by reducing p70 S6 kinase-mediated serine phosphorylation of IRS-1. *J. Biol. Chem.* **282**, 7991–7996 (2007).
44. Houstis, N., Rosen, E. D. & Lander, E. S. Reactive oxygen species have a causal role in multiple forms of insulin resistance. *Nature* **440**, 944–948 (2006).
45. St-Pierre, J. *et al.* Suppression of reactive oxygen species and neurodegeneration by the PGC-1transcriptional coactivators. *Cell* **127**, 397–408 (2006).


**Supplementary Information** is linked to the online version of the paper at www.nature.com/nature.

**Acknowledgements** We thank B. M. Spiegelman for critical discussions and reading of the manuscript; T. Yokomizo for discussion and support; A. Tsuchida, K. Hara, Y. Hada, Y. Nio, T. Maki, T. Takazawa, Y. Iwata, M. Kobayashi, S. Kawamoto, K. Kobayashi, K. Hirota, Y. Shiomi, T. Mitsumatsu, L. Hirose, Y. Sea, M. Nakamura and K. Take for technical help and support; and S. Suzuki, K. Miyata, C. Ueda, A. Itoh and A. Okano for technical assistance. This work was supported by Grant-in-aid for Scientific Research (S) (20229008) (to T.K.), (B) (20390254) (to T.Y.), Targeted Proteins Research Program (to T.K.), the Global COE Research Program (to T.K.) and Translational Systems Biology and Medicine Initiative (to T.K.) from the Ministry of Education, Culture, Sports, Science and Technology of Japan.

**Author Contributions** M.I., M.O.-I., T.Y., K.S., T.N., M.F., M.Y., S.N., R.N., M.T., H.O., N.K., I.T., Y.K.H. and N.Y. performed experiments. T.K. and T.Y. conceived and supervised the study. K.T., T.S. and K.H. supervised the study. T.Y., T.K., M.I. and M.O-I. wrote the paper. All authors interpreted data.

**Author Information** Reprints and permissions information is available at www.nature.com/reprints. The authors declare no competing financial interests. Correspondence and requests for materials should be addressed to T.K. (kadowaki-3im@h.u-tokyo.ac.jp) or T.Y. (tyamau-tky@umin.net).

Cell Metabolism
Article

# Macrophage-Derived AIM Is Endocytosed into Adipocytes and Decreases Lipid Droplets via Inhibition of Fatty Acid Synthase Activity

Jun Kurokawa,[1] Satoko Arai,[1] Katsuhiko Nakashima,[1] Hiromichi Nagano,[1] Akemi Nishijima,[1] Keishi Miyata,[3] Rui Ose,[4] Mayumi Mori,[1] Naoto Kubota,[2] Takashi Kadowaki,[2] Yuichi Oike,[3] Hisashi Koga,[4] Maria Febbraio,[5] Toshihiko Iwanaga,[6] and Toru Miyazaki[1,*]

[1]Laboratory of Molecular Biomedicine for Pathogenesis, Center for Disease Biology and Integrative Medicine, Faculty of Medicine
[2]Department of Internal Medicine, Graduate School of Medicine
The University of Tokyo, Tokyo, 113-0033, Japan
[3]Department of Molecular Genetics, Graduate School of Medical Sciences, Kumamoto University, Kumamoto, 860-8556, Japan
[4]Department of Human Genome Research, Kazusa DNA Research Institute, Kisarazu, Chiba, 292-0818, Japan
[5]Department of Cell Biology, Lerner Research Institute, Cleveland Clinic Foundation, Cleveland, OH 44195, USA
[6]Department of Functional Morphology, Laboratory of Histology and Cytology, Hokkaido University Graduate School of Medicine, Sapporo, Hokkaido, 060-0815, Japan
*Correspondence: tm@m.u-tokyo.ac.jp
DOI 10.1016/j.cmet.2010.04.013

## SUMMARY

**Macrophages infiltrate adipose tissue in obesity and are involved in the induction of inflammation, thereby contributing to the development of obesity-associated metabolic disorders. Here, we show that the macrophage-derived soluble protein AIM is endocytosed into adipocytes via CD36. Within adipocytes, AIM associates with cytosolic fatty acid synthase (FAS), thereby decreasing FAS activity. This decreases lipid droplet size, stimulating the efflux of free fatty acids and glycerol from adipocytes. As an additional consequence of FAS inhibition, AIM prevents preadipocyte maturation. In vivo, the increase in adipocyte size and fat weight induced by high-fat diet (HFD) was accelerated in *AIM*-deficient ($AIM^{-/-}$) mice compared to $AIM^{+/+}$ mice. Moreover, injection of recombinant AIM in $AIM^{-/-}$ mice suppresses the increase in fat mass induced by HFD. Interestingly, metabolic rates are comparable in $AIM^{-/-}$ and $AIM^{+/+}$ mice, suggesting that AIM specifically influences adipocyte status. Thus, this AIM function in adipocytes may be physiologically relevant to obesity progression.**

## INTRODUCTION

It is well known that adipose tissues in obesity are in a state of chronic inflammation (Olshansky et al., 2005; Baker et al., 2007). Accumulating evidence indicates that this inflammation is induced predominantly by the recruitment of a large number of macrophages into adipose tissues (Olshansky et al., 2005; Baker et al., 2007; Apovian et al., 2008). Although the precise mechanism underlying the initiation of macrophage recruitment to adipose tissues remains a matter of debate, adipose tissue macrophage number rapidly increases as obesity progresses (Surmi and Hasty, 2008). The subclinical inflammatory state of adipose tissues is tightly associated with insulin resistance of adipose tissues as well as systemic insulin resistance and cardiovascular disease (Neels and Olefsky, 2006; Shoelson et al., 2006). Thus, adipose tissue macrophages are thought to play key roles in several obesity-induced metabolic disorders. However, whether adipose tissue macrophages also exert direct effect(s) on surrounding adipocytes, independent of inflammatory responses, remains to be determined. To address this question, we focused on the protein AIM (apoptosis inhibitor of macrophage, also known Spα, Api6, and CD5L) in the context of its effects on adipocytes, because AIM is produced and secreted specifically by tissue macrophages, and its expression in vivo is markedly increased with obesity progression in mice (Miyazaki et al., 1999; Arai et al., 2005).

The AIM protein is a member of the scavenger receptor cysteine-rich superfamily (SRCR-SF) and was initially identified as an apoptosis inhibitor that supports the survival of macrophages themselves against various apoptosis-inducing stimuli (Miyazaki et al., 1999). As a secreted molecule, AIM has been detected in human and mouse blood at varying levels (Miyazaki et al., 1999; Gebe et al., 1997, 2000; Gangadharan et al., 2007; Kim et al., 2008; Gray et al., 2009). Based on the observation that *AIM* is a direct target for regulation by nuclear receptor LXR/RXR heterodimers (Joseph et al., 2004; Valledor et al., 2004), we found that AIM is expressed in lipid-laden macrophages at atherosclerotic lesions, and this induction is associated with atherosclerogenesis by supporting the survival of macrophages within lesions (Arai et al., 2005). Other studies have shown that AIM appears to be multifunctional and is effective in cell types other than macrophages, including B and natural killer (NK) T lymphocytes (Yusa et al., 1999; Kuwata et al., 2003) and myeloid cells (Qu et al., 2009). However, the functional nature of AIM remains enigmatic because we are ignorant of the precise mechanism by which it elicits its effects.

In the present study, we assessed the expression of AIM by adipose tissue macrophages in obese mice. We also analyzed how AIM interacts with adipocytes. In addition, an effect of AIM on adipocytes and its consequence with respect to the regulation of adipocyte size in vivo was determined. Finally, we investigated the molecular mechanism underlying this role of AIM in adipocytes. Based on these results, we will discuss the putative role of AIM on the state of adipose tissues.

## RESULTS

### AIM in Adipose Tissue Macrophages in Obese Mice

We first assessed the expression of AIM by adipose tissue macrophages in obese C57BL/6 (B6) mice after the administration of a high-fat diet (HFD) (fat kcal 60%) for 20 weeks. In obese mice, large numbers of macrophages were observed within visceral fat tissues, forming clusters or crown-like structures (CLSs) (Cinti et al., 2005), whereas few adipose tissue macrophages were detected in lean mice (Figure 1A). As shown in Figure 1B, macrophages (stained with F4/80 pan macrophage antibody) in obese adipose tissues showed staining with an antibody specific to AIM (SA-1) (Arai et al., 2005). These AIM-positive macrophages were also positive for interleukin (IL)-6 staining, indicating that they were the inflammatory macrophage type (M1) (Figure 1B). In contrast, F4/80-positive macrophages within adipose tissues from lean mice were negative for AIM and IL-6 staining (Figure 1B). Similarly, the serum level of AIM was increased in obese mice compared to lean mice (Figure 1C). It is possible that AIM detectable in lean mice is derived predominantly from macrophages in other macrophage-containing tissues (Miyazaki et al., 1999; Gebe et al., 2000; Arai et al., 2005). To exclude the possible expression of AIM by adipocytes, adipocytes from epididymal fat tissue of obese mice were fractionated after collagenase treatment (Brake et al., 2006) and assessed for *AIM* expression by quantitative real-time PCR (QPCR). No *AIM* expression was observed in purified adipocytes (Figure S1A). In addition, 3T3-L1 adipocytes were analyzed after the induction of maturation by insulin, dexamethasone (DEX), and isobutylmethylxanthine (IBMX). Again, *AIM* expression was not detectable in mature 3T3-L1 adipocytes (Figure S1B).

### Endocytosis of AIM into Adipocytes

Intriguingly, although we found no *AIM* expression by adipocytes (Figure S1), some adipocytes surrounding adipose tissue macrophages in obese mice showed AIM staining (Figure 2A, arrows). This may indicate a physiologic association of AIM with tissue adipocytes. To test this possibility, we injected recombinant AIM (rAIM) into epididymal fat in obese male $AIM^{-/-}$ mice and analyzed fat tissue histologically 3 hr later. Epididymal fat was selected for this experiment owing to its ease of manipulation. Interaction of AIM with adipocytes was clearly confirmed in $AIM^{-/-}$ mice. As shown in Figure 2B (left and middle lanes), $AIM^{-/-}$ adipocytes were positive for AIM staining when rAIM was injected locally into fat tissue (Figure 2B, left and middle lanes). Staining for AIM was also detected in adipocytes in fat tissue in which rAIM was administered systemically to $AIM^{-/-}$ mice via intravenous (i.v.) injection (Figure 2B, right lane). These results implicate adipocytes as a target cell type for AIM. Macrophages also stained for AIM in $AIM^{-/-}$ adipose tissue after injection of rAIM (Figure 2B), consistent with the fact that AIM is effective in macrophages (Miyazaki et al., 1999; Arai et al., 2005).

To further investigate how AIM interacts with adipocytes, differentiated 3T3-L1 adipocytes were treated with rAIM, and the association of rAIM with these cells was analyzed by confocal microscopy. Interestingly, rAIM accumulated within the cytoplasm of adipocytes, forming many dots within the intracellular compartment (Figure 3A). After stimulation with insulin, DEX, and IBMX, a large proportion of 3T3-L1 cells underwent differentiation, expressing peroxisome proliferator-activated receptor γ 2 (PPARγ2) at a high level, whereas some cells remained in an undifferentiated state, expressing PPARγ2 at a low or undetectable level (Madsen et al., 2003). As shown in Figure 3A, among this heterogeneous cell population, mature adipocytes strongly positive for PPARγ2 (yellow arrows) efficiently incorporated rAIM, whereas adipocytes faintly positive for PPARγ2 (blue arrows) or negative (white arrows) did not (left and middle lanes). Preadipocytes not stimulated by insulin, DEX, and IBMX did not incorporate rAIM (Figure 3A, right lane). As shown in Figure 3B, incorporated rAIM colocalized with early endosomes (positive for early endosome antigen 1; EEA1) but not with late endosomes (positive for Rab7) or recycling endosomes (positive for Rab11). These results suggest that incorporated AIM was transported to the cytosol during endosome maturation. No costaining for AIM and lysosomes or lipid droplets was observed (Figure 3B; AIM + lysosome, AIM + lipid droplets). Additional analysis of the cells by electron microscopy shown may support the specific colocalization of AIM with endosomes (Figures 3C and S2). Gold particles indicating rAIM immunoreactivity were mainly associated with endosome-like structures, where the limiting membrane of the structures and the periphery of their contents were heavily labeled (Figure 3C). Endocytosis of rAIM was observed at the cell membrane (Figure 3C, indicated by arrows). Other organelles were essentially negative for AIM immunolabeling (Figure S2). All these data suggest that AIM is incorporated into adipocytes via endocytosis, is transported to the cytoplasm, and function intracellularly.

### Cell-Surface CD36-Mediated Internalization of AIM

The accumulation of AIM at the membrane of endosome-like particles (Figure 3C) indicates that the internalization of exogenous AIM may be mediated by a cell-surface molecule. As a candidate molecule responsible for endocytosis, we focused on scavenger receptor CD36 because it promotes the internalization of various molecules, including lipoproteins and fatty acids (Greenwalt et al., 1992; Ibrahimi and Abumrad, 2002), and it is expressed by adipocytes and macrophages, which are target cells for AIM. Thus, we assessed whether treatment of 3T3-L1 adipocytes with a neutralizing antibody against CD36 (clone JC63.1; mouse IgA) interfered with rAIM uptake. As shown in Figure 3D, incorporation of rAIM was drastically decreased in the presence of this neutralizing antibody. In addition, we injected rAIM intravenously into $CD36^{-/-}$ (Febbraio et al., 1999) and $CD36^{+/+}$ mice and analyzed the incorporation of rAIM into adipose tissues. As shown in Figure 3E, incorporation of rAIM into adipocytes was markedly less in $CD36^{-/-}$ mice compared to $CD36^{+/+}$ mice. These data strongly indicate that CD36 is responsible for AIM internalization. This was also supported by microscopic analysis of the association of rAIM

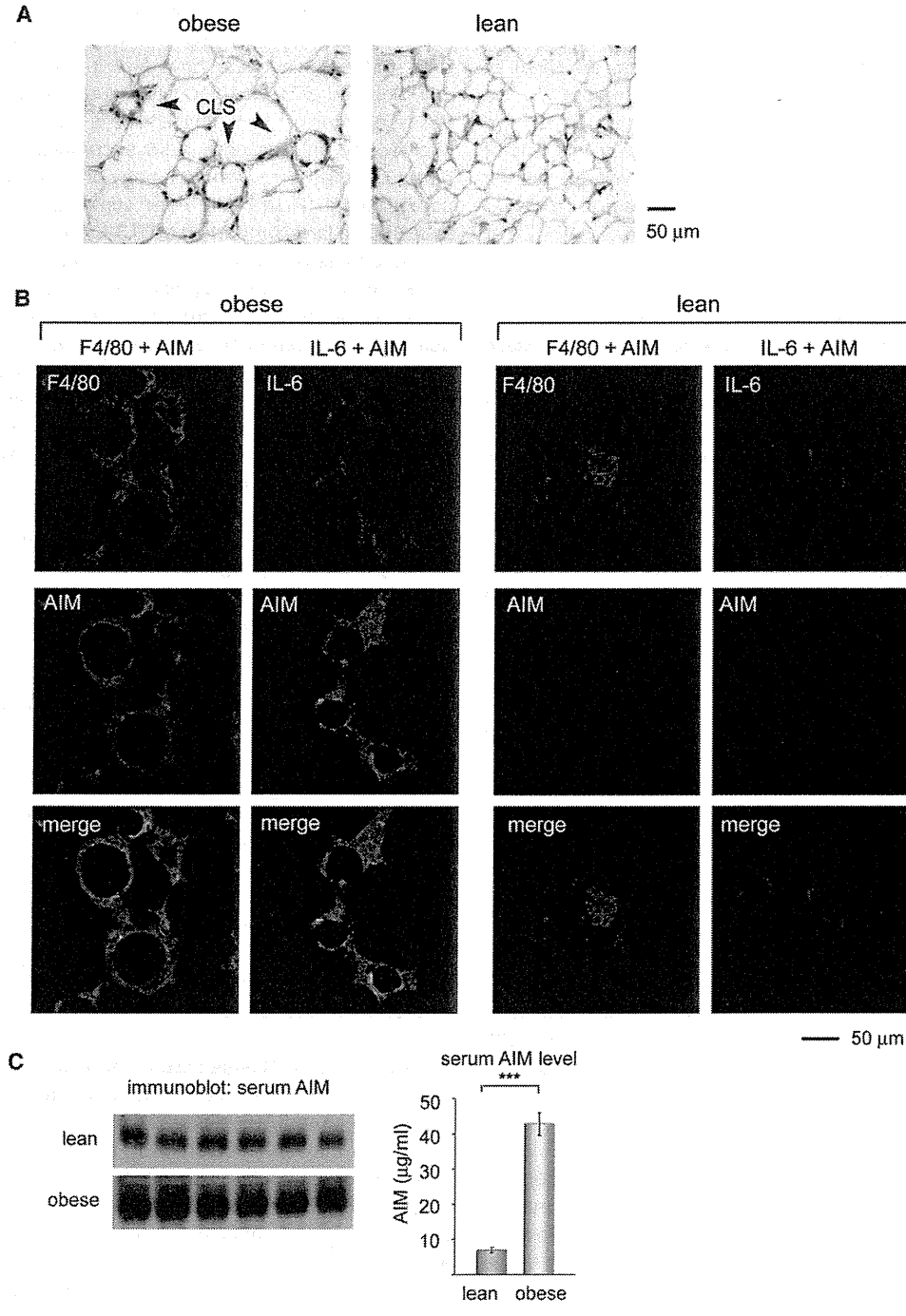


**Figure 1. Immunohistochemical Analysis of AIM in Adipose Tissues**

(A) Representative photomicrographs of visceral fat tissue from lean (fed with normal chow) or obese (fed with a HFD for 20 weeks) wild-type B6 mice stained with hematoxylin and eosin (H&E). The crown-like structures (CLSs) formed by recruited macrophages are indicated by arrows.

(B) Specimens of visceral fat tissues from lean or obese B6 mice were costained for AIM (green) and F4/80 (pan macrophage marker; red) or AIM (green) and IL-6 (red).

(C) Immunoblotting for serum AIM. A volume of 1 μl of serum from six separate lean (fed with normal chow) or obese (fed with a HFD for 20 weeks) mice was used. Results for immunoblots and actual AIM concentration are presented. AIM concentration was calculated by comparison with the density obtained with various amounts of recombinant AIM (rAIM) on the same blot. The density of the signal was calculated using image analysis software NIH ImageJ. Error bar indicates SEM.

with Flag-tagged mouse CD36 expressed on the surface of HEK293T cells. Notably, the accumulation of rAIM staining (green) was specifically colocalized with Flag-CD36 (red) on the cell surface (Figure S3).

### AIM Decreases Adipocyte Lipid Droplet Size

We next assessed the effect of incorporated AIM in host adipocytes. To achieve this, differentiated 3T3-L1 adipocytes in culture (at 4 days after maturation stimulation) were challenged

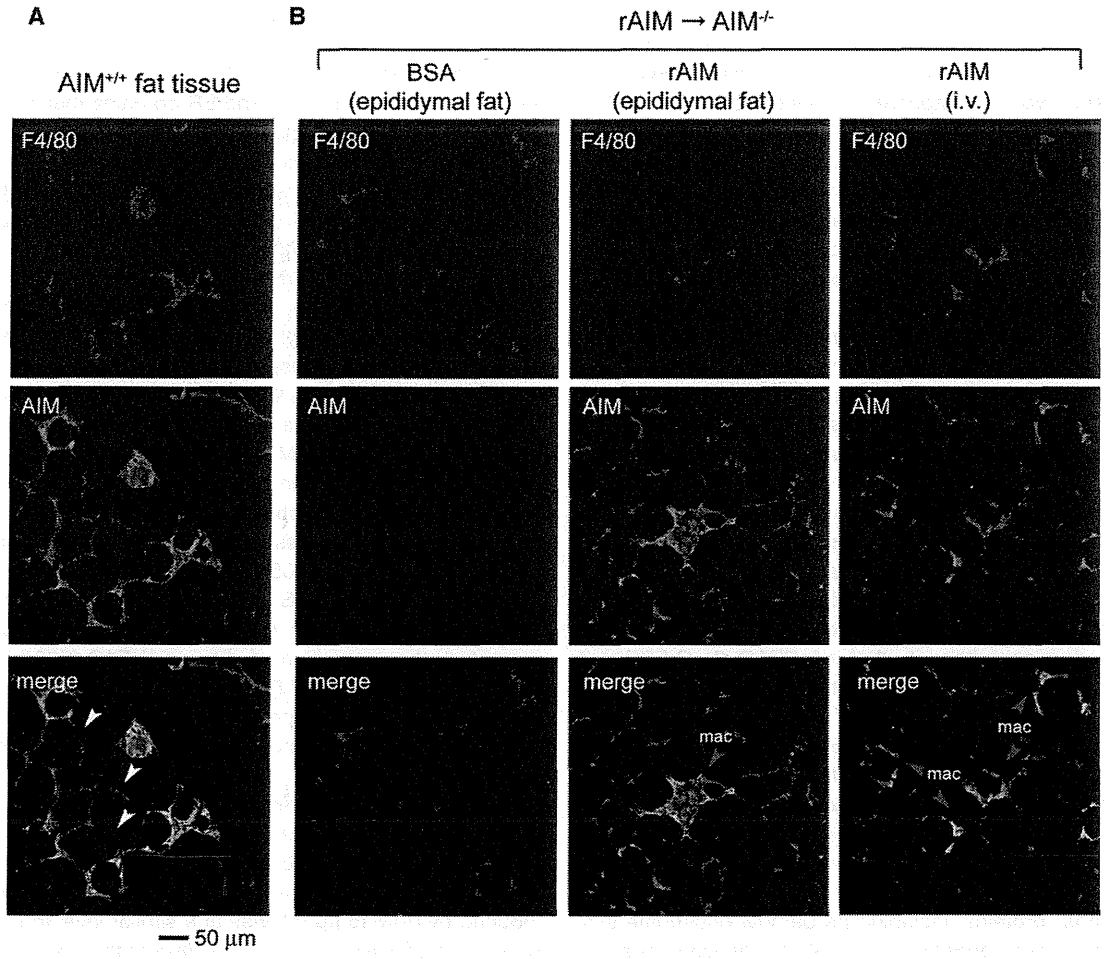


**Figure 2. Association of Exogenous AIM with Adipocytes**

(A) Epididymal fat sections were stained for AIM (green) and F4/80 (red). Staining for AIM was detected in macrophages and some adipocytes (arrows).

(B) Uptake of rAIM by $AIM^{-/-}$ adipocytes in vivo. $AIM^{-/-}$ mice were injected with rAIM (middle lane) or BSA (left lane) directly into the epididymal fat (total 100 μg for each at several loci) or with rAIM systemically (300 μg) via i.v. injection (right lane). Three hours after injection, tissue sections were generated and stained for AIM (green) and macrophage F4/80 (red). mac: macrophage.

with rAIM. Remarkably, the size of lipid droplets within the cells was decreased after a 6 day incubation of cells with rAIM (Figure 4A). In addition, the number of cells containing lipid droplets was also decreased (Figure 4A). Supernatant viscosity was also markedly enhanced by the administration of rAIM. These results suggest that rAIM induced a lipolytic response, resulting in the liberation of droplet components such as glycerol and fatty acids from the cells (Zechner et al., 2005; Duncan et al., 2007). We tested this possibility by determining the efflux of glycerol and free fatty acids (FFAs) on days 2, 4, and 6 after stimulation with rAIM. As shown in Figure 4B, the amount of glycerol and FFAs in the supernatant increased significantly when adipocytes were maintained in rAIM. In vivo, basal levels of FFA and glycerol in serum were lower in $AIM^{-/-}$ obese mice than in $AIM^{+/+}$ obese mice (Figure 4C), consistent with the in vitro results.

mRNA levels for *fat-specific protein 27* (*FSP27*, also termed *cidec*), *Perilipin*, and *Adipophilin*, important elements involved in the formation of lipid droplets (Ducharme and Bickel, 2008; Puri and Czech, 2008), were decreased after treatment of 3T3-L1 adipocytes with rAIM (Figure 4D). A significant decrease in these mRNA levels was already apparent 2 days after challenge with rAIM (Figure 4D), consistent with the progression of lipolysis, as reported previously (Zechner et al., 2005; Nishino et al., 2008). In contrast, mRNA level of mature adipocyte markers such as *PPARγ2*, *CCAAT-enhancer-binding protein α* (*C/EBPα*), and *glucose transporter 4* (*GLUT4*) and an immature adipocyte marker, *Preadipocyte factor-1* (*PREF-1*) (Smas and Sul, 1993), was not remarkably changed in response to rAIM treatment, suggesting that rAIM did not appear to induce dedifferentiation of adipocytes (Figure 4D). Local injection of rAIM into epididymal fat tissue of $AIM^{-/-}$ mice resulted in similar changes in mRNA levels of these genes (Figure 4E).

### Increase in Adipocyte Size and Adipose Tissue Mass in $AIM^{-/-}$ Mice

Consistent with the observations in 3T3-L1 cells, the size of visceral fat adipocytes was larger in obese $AIM^{-/-}$ mice than in obese $AIM^{+/+}$ mice (Figure 5A). Relevant to this enlargement of

adipocytes, the increase in weight of both visceral and subcutaneous fat tissues in mice fed with a HFD (12 weeks) was more accelerated in $AIM^{-/-}$ mice than in $AIM^{+/+}$ mice (Figure 5B). This difference was also apparent in mice fed with a HFD for a longer period (20 weeks) (Figure S4). It is noteworthy that $AIM^{-/-}$ mice and $AIM^{+/+}$ mice fed with a HFD showed comparable metabolic rates (e.g., body temperature, oxygen consumption, and food intake) (Figure S5). Locomotor activity was also equivalent in both types of mice (Figure S5). Thus, AIM appears to influence adipose tissue mass by specifically affecting adipocytes.

We also injected rAIM intraperitoneally (twice a week) into $AIM^{-/-}$ mice fed with a HFD for 5 weeks to assess whether rAIM administration might suppress the increase in adipose tissue mass. As expected, the increase in weight of whole-body as well as both visceral and subcutaneous fat tissues was significantly less in mice injected with rAIM than in those injected with bovine serum albumin (BSA) (Figure 5C). As observed for the treatment of 3T3-L1 adipocytes with rAIM (Figure 4D), mRNA levels of *FSP27*, *Perilipin*, and *Adipophilin* were also lower in the epididymal adipose tissue in mice injected with rAIM (Figure 5D). Interestingly, mRNA level of *PREF-1* was higher in rAIM-injected mice, although that of *PPARγ2*, *C/EBPα*, or *GLUT4* was similar in mice injected with rAIM or BSA (Figure 5D).

### AIM Decreased Fatty Acid Synthase Activity

We were interested in the intracellular target molecule(s) of incorporated AIM in adipocytes. To this end, we performed immunoprecipitation-mass spectrometry (IP-MS) analysis with lysates from different cells and tissues. Fatty acid synthase (FAS) was identified as a candidate molecule with the potential to associate with AIM (other proteins, including carbamoyl phosphate synthase-1, major vault protein, and aldehyde dehydrogenase 1 family member L1, were also associated with AIM; complete results of this analysis will be published elsewhere). FAS is highly expressed in adipose tissues and catalyzes the synthesis of saturated fatty acids, such as palmitate, from acetyl-CoA and malonyl-CoA precursors. Accumulating evidence has highlighted critical roles of FAS in a variety of biological aspects, including early embryogenesis (Chirala et al., 2003), in addition to providing a metabolic substrate. A number of biochemical and genetic studies have suggested the involvement of FAS in the regulation of adipose tissue mass (Loftus et al., 2000; Makimura et al., 2001; Kumar et al., 2002; Mobbs and Makimura, 2002; Shimokawa et al., 2002; Kovacs et al., 2004; Liu et al., 2004; Ronnett et al., 2005; Schmid et al., 2005; Chakravarthy et al., 2009a).

We confirmed the association of AIM and FAS in vivo and in vitro. After injecting rAIM into epididymal fat of obese $AIM^{-/-}$ mice, we precipitated incorporated rAIM from fat tissue lysates and addressed whether endogenous FAS was also precipitated. As shown in Figure 6A, the proteins coprecipitated, confirming the association of incorporated AIM and cytosolic FAS. In addition, a coimmunoprecipitation (coIP) assay with HEK293T cells expressing Flag-tagged FAS and HA-tagged AIM showed that the two proteins coprecipitated, indicating that AIM possesses the potential to bind to FAS (Figure 6B).

We also attempted to map FAS-binding region(s) for AIM. FAS consists of seven discrete functional domains: ketoacyl synthase (KS), malonyl/acetyl transferase (MAT), dehydrase (DH), enoylreductase (ER), ketoreductase (KR), acyl carrier protein (ACP), and thioesterase (TE) (Smith, 1994). There is a central core (CC) between the DH and ER domains that has no known catalytic function and may play a structural role in stabilizing the dimer (illustrated in schematic in Figure 6C). We assessed the association of HA-tagged AIM with each FAS region tagged with a Flag sequence by coIP assay. Notably, AIM bound specifically to ER, DH, TE, and CC domains, but not to the N-terminal region containing KS and MAT, which are involved in the initial acyl chain assembly (i.e., condensation of acetyl and malonyl moieties to 3-ketobutyryl-ACP along with the release of $CO_2$) (Figures 6C and S6). Thus, AIM appears to influence the elongation of fatty acid chains (which involves ER and DH) and the release of synthesized palmitate (which is dependent on TE).

The association of AIM with the CC domain suggested that AIM might also affect the dimerization of FAS. It is well known that FAS is highly functional as a dimerized form, whereas monomeric FAS possesses little or no activity (Smith et al., 1985; Asturias et al., 2005). Therefore, we analyzed the dimer/monomer status of FAS protein in 3T3-L1 adipocytes after culture in the presence or absence of rAIM for 6 days. As expected, the proportion of dimerized FAS (500 kDa) (as assessed by separation of FAS on a Tris-acetate gel specific for large molecular weight proteins) was significantly less in cells maintained in the presence of rAIM than in cells without rAIM treatment (Figure 6D).

Consistent with these results, the enzymatic activity of FAS (as assessed by the consumption of malonyl-CoA) (Kelley et al., 1986) was markedly decreased in 3T3-L1 adipocytes treated with rAIM as above (Figure 6E). The decrease in FAS activity induced by rAIM (5 μg/ml) was at a similar level to that induced by C75, a specific FAS inhibitor (Kuhajda et al., 2000), when used at a functional concentration (25 μM) (Figure 6E). In vivo, FAS activity was significantly increased in epididymal fat of $AIM^{-/-}$ mice compared to that of $AIM^{+/+}$ mice (Figure 6F). In addition, supplementation of rAIM via direct injection decreased FAS activity in epididymal fat of $AIM^{-/-}$ mice (Figure 6G).

### AIM and FAS Inhibitor C75 Showed Comparable Effects on Adipocytes

To address whether the effect of AIM on adipocytes resulted from the suppression of FAS activity, we tested whether treatment of 3T3-L1 adipocytes with AIM or FAS inhibitor C75 had similar consequences. As expected, rAIM (5 μg/ml) and C75 (25 μM) induced an increase in the efflux of glycerol and FFAs at comparable levels (Figure 7A). We also assessed the influence of AIM on adipogenesis, because Schmid et al. (2005) reported that inhibition of FAS prevented preadipocyte differentiation. Interestingly, the presence of rAIM during stimulation by insulin, DEX, and IBMX (48 hr) completely prevented differentiation of 3T3-L1 preadipocytes toward mature adipocytes at a level equivalent to that observed with C75 (Figure 7B). The numbers of dead cells did not increase in the presence of rAIM at different time points, as assessed by staining with trypan blue or propidium iodide (data not shown). This excludes the argument that rAIM might induce death of 3T3-L1 cells, appearing to decrease the overall number of mature adipocytes. In addition, AIM did not simply attenuate either (or all) of the three stimulators via

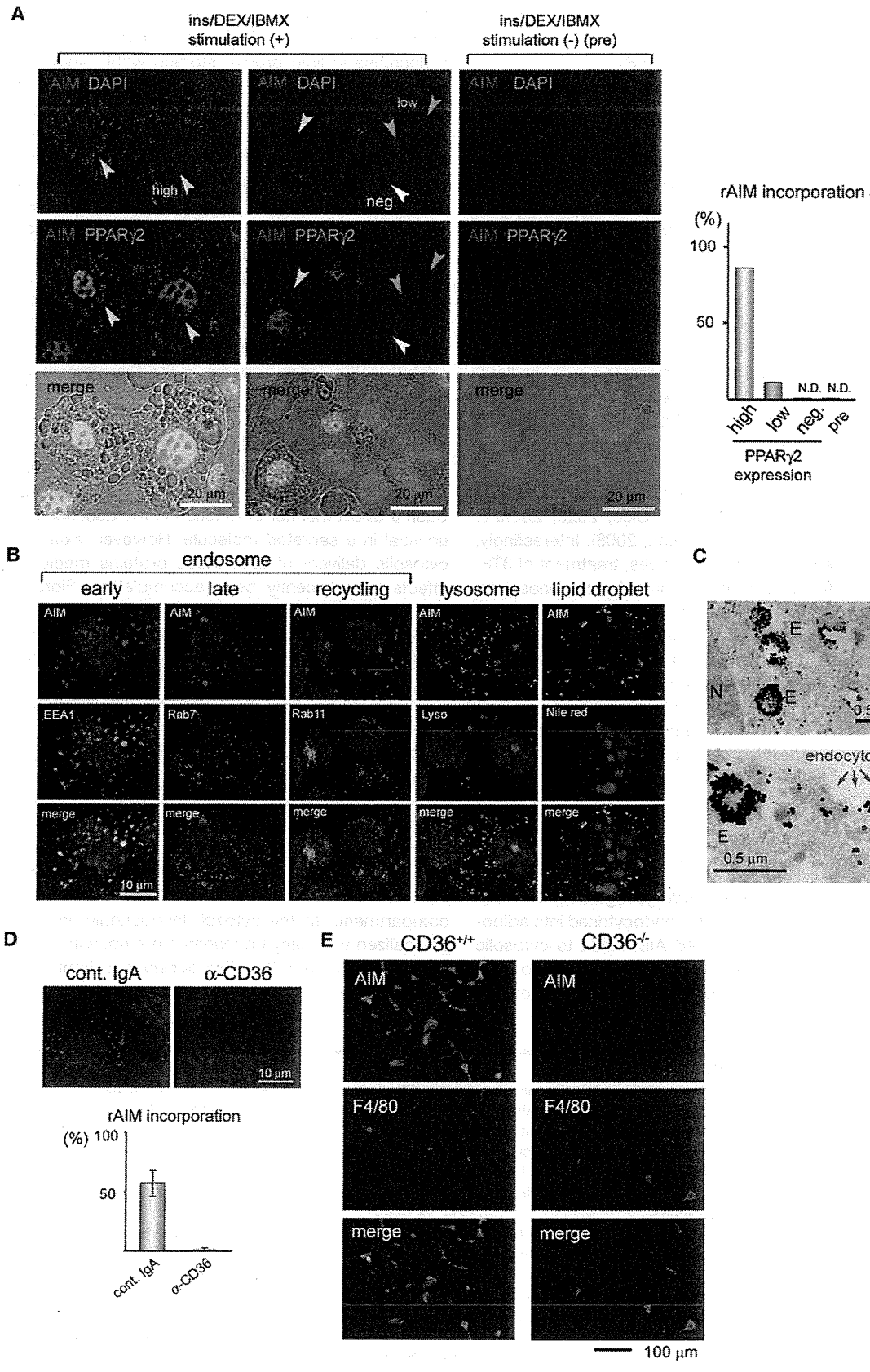
A
ins/DEX/IBMX stimulation (+)
ins/DEX/IBMX stimulation (-) (pre)
AIM DAPI
high
low
neg.
AIM PPARγ2
merge
20 μm
rAIM incorporation
(%)
100
50
N.D. N.D.
high
low
neg.
pre
PPARγ2 expression
B
endosome
early
late
recycling
lysosome
lipid droplet
AIM
EEA1
Rab7
Rab11
Lyso
Nile red
merge
10 μm
C
E
N
0.5 μm
endocytosis
D
cont. IgA
α-CD36
10 μm
rAIM incorporation
(%) 100
50
cont. IgA
α-CD36
E
CD36+/+
CD36-/-
AIM
F4/80
merge
100 μm

chemical interaction; coincubation with rAIM followed by removal of rAIM via column purification did not alter their ability to induce 3T3-L1 cell differentiation (Figure S7).

Consistent with these morphologic results, cells cultured in the presence of rAIM or C75 showed a marked decrease in mRNA levels of *C/EBPα* and *PPARγ* (*γ1* and *γ2*), the master regulator genes for adipogenesis (Rosen et al., 1999; Wu et al., 1999a; Farmer, 2006), as well as of downstream genes characteristic of functional adipocytes, such as *CD36* and *GLUT4*, compared to cells differentiated in the absence of rAIM or C75 (Figure 7C). Altogether, these results indicate that AIM affected adipocytes by inhibiting FAS activity.

### Inhibition of FAS Did Not Activate cAMP-Dependent Lipolysis

During periods of energy deprivation, adipocytes undergo lipolysis via stimulation of a G protein-coupled receptor/cyclic AMP (cAMP)-dependent signaling cascade, followed by phosphorylation of protein kinase A (PKA), which activates hormone-sensitive lipase (HSL). At the same time, the level of *adipose triglyceride lipase* (*ATGL*) mRNA also increases (Wu et al., 1999b; He et al., 2003; Holm, 2003; Finn and Dice, 2006; Zechner et al., 2005; Duncan et al., 2007; Lafontan, 2008). Interestingly, however, despite the lipolytic consequences, treatment of 3T3-L1 adipocytes with rAIM or C75 did not upregulate the phosphorylation of PKA (Figure S8A). In addition, the levels of *ATGL* and *HSL* mRNA did not increase in response to AIM (Figure S8B). Thus, unlike in a starved situation, inhibition of FAS does not stimulate cAMP/PKA-dependent lipolysis. Note that the level of phosphorylation of 5′-AMP-activated kinase (AMPK), another element downstream of cAMP signaling whose activation inhibits HSL activity, was also not increased by AIM or C75 (Figure S8C).

## DISCUSSION

### A Role of AIM in Adipocytes

Our present results provide several findings regarding the influence of AIM on adipocytes. First, AIM is endocytosed into adipocytes via CD36. Second, incorporated AIM binds to cytosolic FAS protein at various regions responsible for elongation of fatty acids, release of synthesized palmitate, and stabilization of FAS dimerization. This results in a decrease in FAS enzymatic activity. Third, the decrease in FAS activity induced by AIM results in a decrease in lipid droplet storage within adipocytes. Finally, the size of adipocytes in visceral fat tissue is increased in $AIM^{-/-}$ mice compared to $AIM^{+/+}$ mice. The physiologic consequence of the lipolytic response induced by AIM remains to be investigated. It is possible that AIM resists augmentation of adipose tissue mass, leading to decreased progression of obesity. Indeed, the increase in weight of visceral fat in mice fed with a HFD was accelerated in $AIM^{-/-}$ mice compared to $AIM^{+/+}$ mice (Figure 5B), and it was suppressed by the systemic administration of rAIM (Figure 5C). Importantly, this antiadiposity function of AIM appears to be exerted specifically via its effect on adipocytes, because both $AIM^{-/-}$ and $AIM^{+/+}$ mice showed comparable metabolic rates (Figure S5). Additional discussion related to this issue appears in the Supplemental Information online.

### Direct Function of AIM in the Absence of Signaling

Interestingly, exogenous AIM secreted by macrophages is incorporated into adipocytes and directly functions intracellularly. Such a direct manner of function in the absence of signaling is unusual in a secreted molecule. However, examples in which cytosolic delivery of exogenous proteins mediates biological effects have recently been accumulating. Fibroblast growth factor (FGF)-1 and -2 (Olsnes et al., 2003; Wesche et al., 2006) as well as epidermal growth factor (EGF) (Lin et al., 2001) are transported to the cytosol after internalization via specific receptors, where they trigger cellular events. In addition, many plant and bacterial toxins, such as ricin and Shiga toxin, are also endocytosed by eukaryotic cells in a receptor-dependent manner and are translocated into the cytosol to target-specific intracellular proteins (Sandvig and van Deurs, 2000, 2005). It is also known that in dendritic cells, some exogenous antigens can access the cytosol via similar machineries for intracellular transport and are presented by major histocompatibility complex (MHC) class I (Ackerman et al., 2005; Giodini and Cresswell, 2008). Yet it remains unclear how AIM is translocated from endosomal compartments to the cytosol. Interestingly, incorporated AIM colocalized with early endosomes but not with late or recycling endosomes (Figure 3B). This observation implicates the presence of a specific mechanism to transport AIM from endosomes

**Figure 3. AIM Is Endocytosed via CD36**

(A) Differentiated 3T3-L1 adipocytes (ins/DEX/IBMX stimulation +) or undifferentiated 3T3-L1 preadipocytes without maturation stimulation (ins/DEX/IBMX stimulation −) were incubated with rAIM (5 μg/ml) for 3 hr and stained for AIM (red), PPARγ2 (green), and DAPI (blue). Top panels, AIM + DAPI; middle panels, AIM + PPARγ2; bottom panels, AIM + PPARγ2 + DAPI (merged), overlaid with phase-contrast images. In the bottom panels, cells showing strong PPARγ2 positivity contained many lipid droplets. Yellow arrows, mature 3T3-L1 adipocytes showing strong staining for PPARγ2; blue arrows, cells showing faint staining for PPARγ2; white arrows, cells showing undetectable staining for PPARγ2. Right lane (pre): undifferentiated 3T3-L1 preadipocytes without stimulation. The percentage of cells showing AIM incorporation was calculated for 100 cells of each type (graph under photomicrographs; rAIM incorporation). Results were obtained from three independent experiments.

(B) 3T3-L1 adipocytes treated with rAIM for 3 hr were costained for AIM (red) and early, late, or recycling endosomes (green: with antibody to EEA1, Rab7, or Rab11, respectively); AIM (green) and lysosomes (red: LysoTracker Red DND-99); and AIM (green) and lipid droplets (red: Nile Red). Specimens were observed under a confocal microscope.

(C) Electron microscopic analysis of the same cell samples after immunogold labeling of AIM. E, endosome; N, nucleus. Scales are indicated by bars.

(D) Treatment of 3T3-L1 adipocytes with CD36-neutralizing antibody inhibited endocytosis of rAIM. Incorporation of rAIM was assessed in cells treated with α-CD36 antibody or control mouse IgA. A total of 100 cells were evaluated for each treatment. Results were obtained from three independent experiments.

(E) Defective uptake of AIM by $CD36^{-/-}$ adipocytes. rAIM (300 μg/mouse in phosphate-buffered saline) was i.v. injected into $CD36^{+/+}$ and $CD36^{-/-}$ mice. At 16 hr after injection, mice were sacrificed and sections were prepared from epididymal fat tissue. Sections were stained for AIM (green: upper panels) and macrophages F4/80 (red: middle panels).

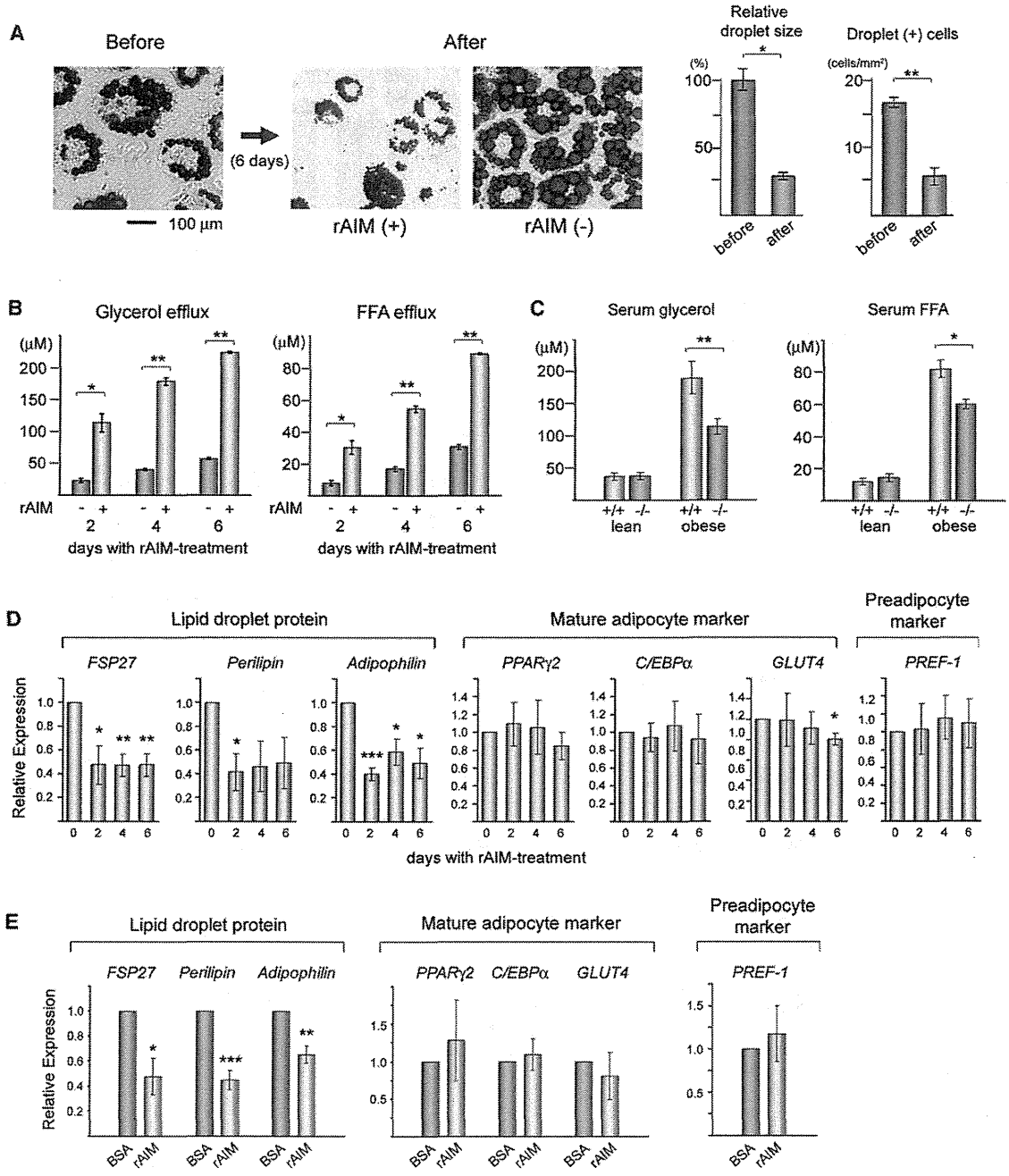


**Figure 4. AIM Induces a Lipolytic Response**

(A) Differentiated 3T3-L1 adipocytes were challenged with rAIM (5 μg/ml) for 6 days. Cells were stained with Oil Red O before and after rAIM treatment. Representative photomicrographs of cells before and after treatment with or without rAIM (5 μg/ml) are presented. Relative droplet size was assessed by evaluating the diameter of 50 droplets. Error bar indicates SEM. The numbers of droplet-containing cells are also shown (cells/mm$^2$). Data are presented as the means of five independent areas. Error bar indicates SEM. Before, before rAIM treatment; After, after 6 day rAIM treatment.

(B) Efflux of glycerol and FFAs after culture of 3T3-L1 adipocytes with or without rAIM (5 μg/ml) for 2, 4, or 6 days. Data are shown as culture supernatant concentrations. Three independent experiments were performed. Error bar indicates SEM.

(C) Basal levels of glycerol and FFAs in serum from lean (fed with normal chow) and obese (fed with a HFD for 20 weeks) *AIM*$^{+/+}$ and *AIM*$^{-/-}$ mice. n = 6 for each group. Error bar indicates SEM.

(D) 3T3-L1 adipocytes incubated with rAIM (5 μg/ml) for 0, 2, 4, or 6 days were analyzed for mRNA levels of *FSP27*, *Perilipin*, *Adipophilin*, *PPARγ2*, *C/EBPα*, *GLUT4*, and *PREF-1* by quantitative PCR. Values were normalized to those of *glyceraldehyde 3-phosphate dehydrogenase* (*GAPDH*) and presented as relative expression to that for the 0 day rAIM treatment. Three independent experiments were performed. Error bar indicates SEM.

(E) In vivo experiment. The mRNA levels of the same genes as in (D) were assessed by QPCR with RNA isolated from epididymal fat in *AIM*$^{-/-}$ mice after direct injection of rAIM (100 μg/whole tissue) or BSA (same amount) into the fat tissues (n = 7 for each). Values were normalized to those of *GAPDH* and presented as relative expression to that from fat tissues injected with BSA. Error bar indicates SEM.

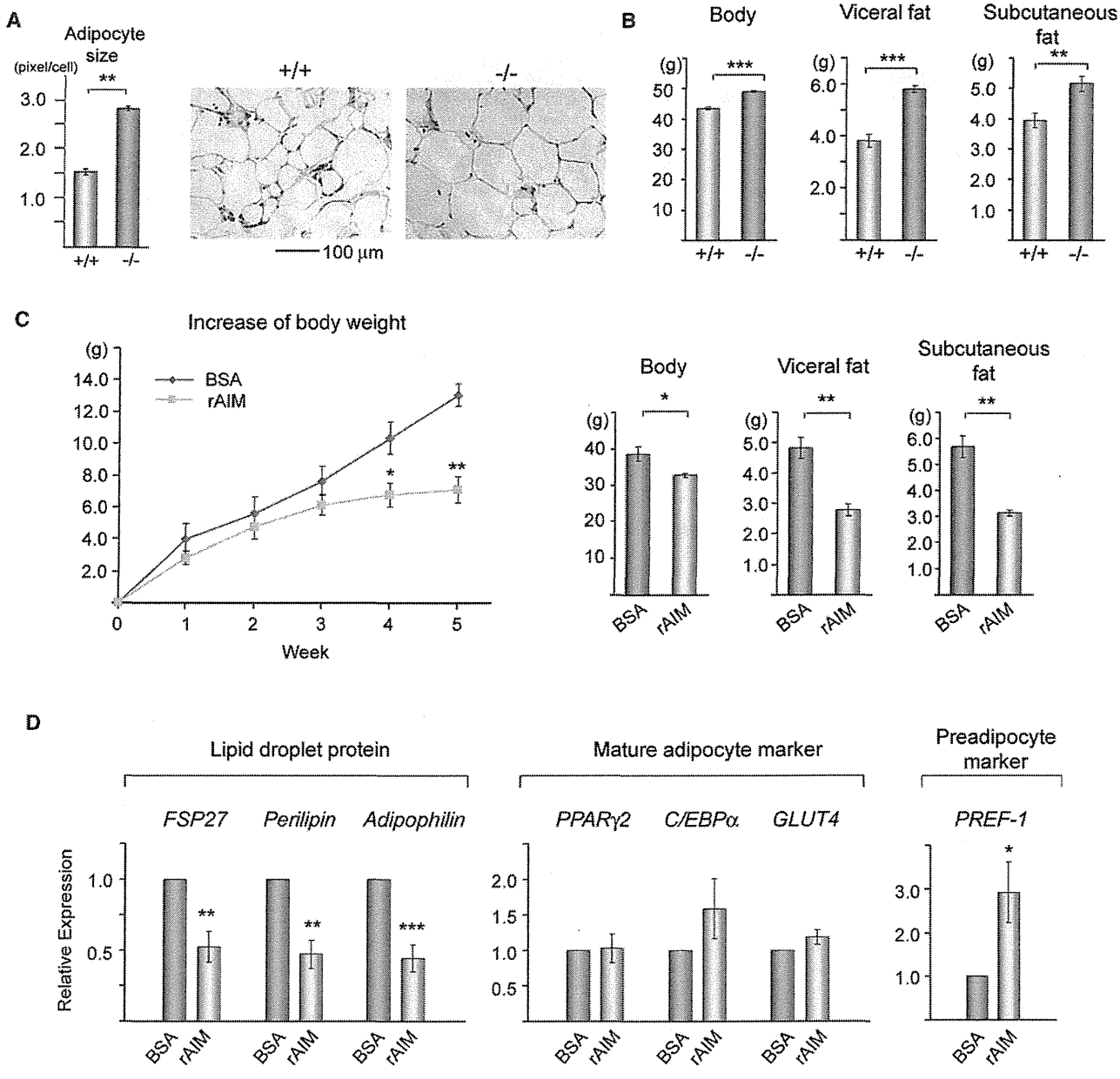


**Figure 5. AIM Influences Adipose Tissue Mass**

(A) Adipocyte size. In $AIM^{+/+}$ mice (+/+) and $AIM^{-/-}$ mice (−/−) (both fed with a HFD for 20 weeks), epididymal fat sections were stained with H&E, and the diameter of 50 independent adipocytes in different areas was evaluated. Results are presented as averages ± SEM (in pixels). Representative photomicrographs of adipose tissues are also presented.

(B) Weights for body, visceral fat tissue, and subcutaneous fat tissue from $AIM^{+/+}$ mice (+/+) and $AIM^{-/-}$ mice (−/−) fed with a HFD for 12 weeks. n = 7 for $AIM^{+/+}$, and n = 6 for $AIM^{-/-}$. Error bar indicates SEM.

(C) $AIM^{-/-}$ mice were fed with a HFD for 5 weeks, and during the period, they were i.p. injected with rAIM or BSA twice a week (300 μg/injection/mouse). The increase in body weight at each week (line graph) and overall body weight and weight of visceral and subcutaneous fat tissues at the end of experiment (bar graphs) are presented. n = 6 for rAIM-injected mice, and n = 5 for BSA-injected mice. Error bar indicates SEM.

(D) mRNA levels of *FSP27*, *Perilipin* and *Adipophilin*, *PPARγ2*, *C/EBPα*, *GLUT4*, and *PREF-1* were assessed by QPCR with RNA isolated from epididymal fat from mice used in (C) at the end of the experiment. Values were normalized to those of *GAPDH* and presented as relative expression to that of fat tissue injected with BSA. n = 6 for rAIM-injected mice and n = 5 for BSA-injected mice. Error bar indicates SEM.

to the cytoplasm. It is possible that a certain cytosolic chaperone is required, as it has recently been found that the efficient translocation of some proteins across the endosomal membrane is dependent on Hsp90 (Haug et al., 2003; Ratts et al., 2003; Wesche et al., 2006; Giodini and Cresswell, 2008). Additional experiments are necessary to clarify the mechanism responsible for AIM translocation from the endosomal compartment to the cytosol.

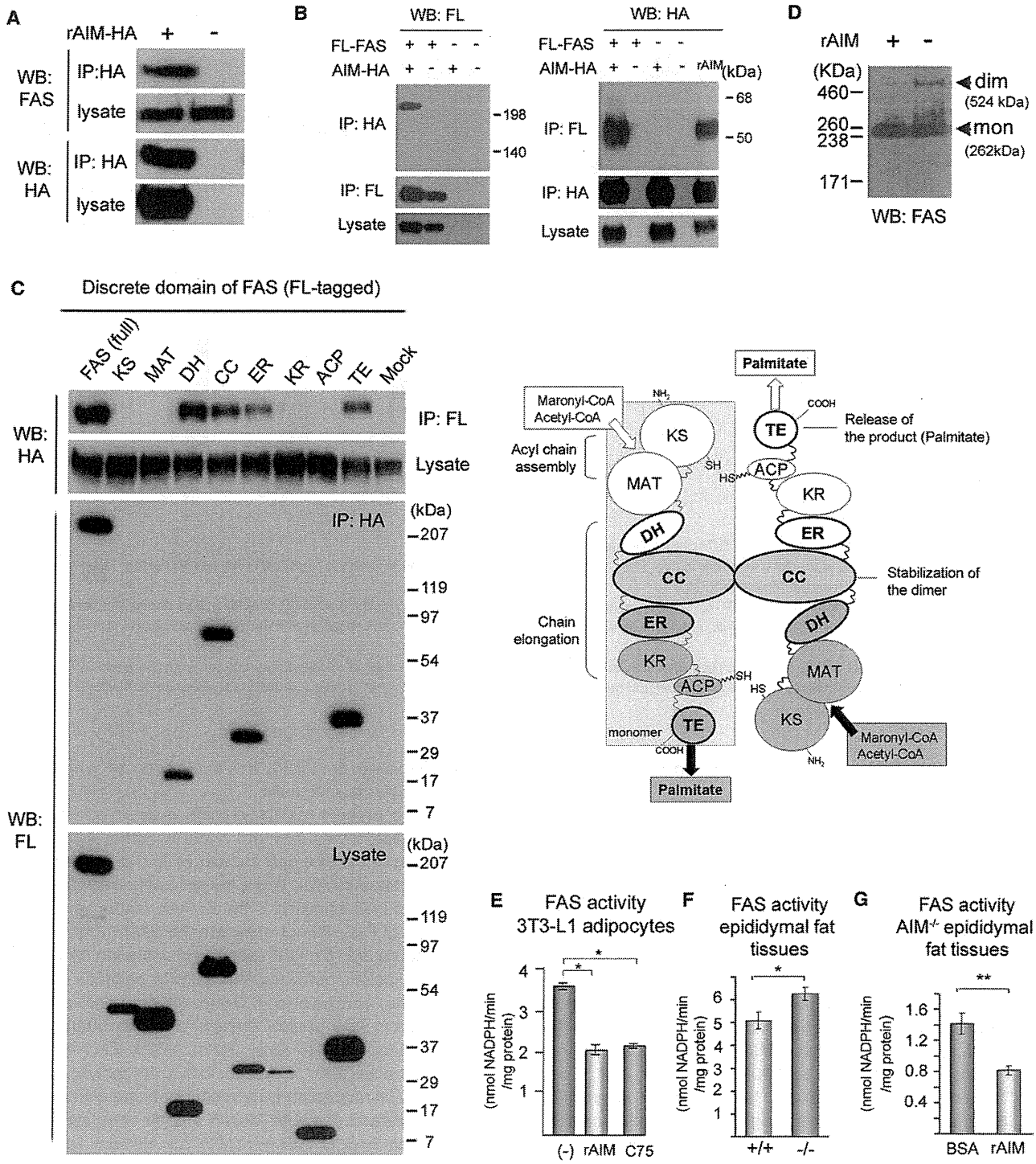


**Figure 6. AIM Targets FAS**

(A) *AIM*$^{-/-}$ mice were injected with rAIM (HA tagged) directly into the epididymal fat (total 100 μg at several loci). Three hours after injection, fat tissues were used to test the association of incorporated rAIM-HA and endogenous cytosolic FAS in fat tissues via coIP using anti-HA antibody. Precipitates were analyzed for the presence of FAS by western blotting (WB).

(B) Association of rAIM (HA tagged) and FAS (FLAG tagged) in HEK293T cells as determined by coIP assay using anti-Flag or anti-HA antibody.

(C) Left: Each domain of FAS was tagged with the Flag sequence at the N terminus and expressed in HEK293T cells stably expressing AIM-HA, and their association was determined by a coIP assay using anti-Flag or anti-HA antibody. Overexpression of ER or KR domains of FAS resulted in death of a large number of cells. This caused a decrease in WB signals using these cell lysates (lower panels, lanes ER and KR). Results from IP-FL/WB-FL, IP-HA/WB-HA, and IP-control IgG (rat or mouse)/WB-FL or -HA are presented in Figure S6. Right: A schematic of head-to-tail dimerized FAS and descriptions of the major function for each region. Two functional units (distinguished by white and gray) are located on the axis of bound CCs. The AIM-binding domains (DH, CC, ER, and TE) are indicated

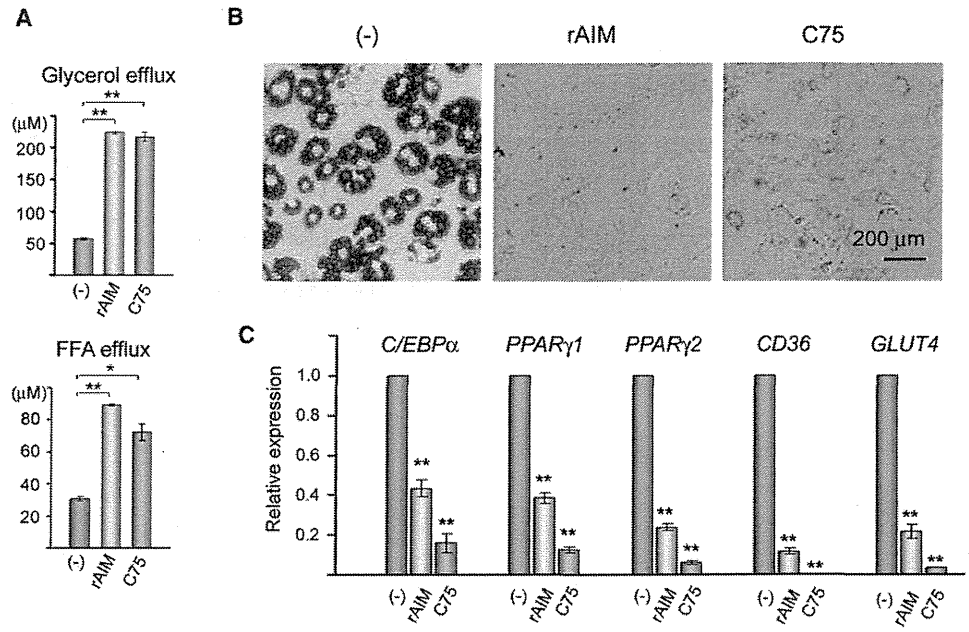


**Figure 7. AIM and C75 Exert Comparable Effects on Adipocytes**

(A) rAIM (5 μg/ml) or C75 (25 μM) was added to differentiated 3T3-L1 adipocytes for 6 days, and the efflux of glycerol and FFAs was evaluated. Three independent experiments were performed. Error bar indicates SEM.

(B) Both AIM and C75 inhibited adipogenesis. 3T3-L1 preadipocytes were challenged with rAIM (5 μg/ml) or C75 (25 μM) for 2 days during stimulation of differentiation by insulin, DEX, and IBMX. At day 12 of culture, cells were stained with Oil Red O. In the presence of rAIM or C75, adipocyte differentiation was completely prevented.

(C) Gene expression profiles at day 12 of culture. Total RNA was isolated from cells, and the mRNA levels for the indicated genes were assessed by QPCR (n = 3 for each group). Values were normalized to those of *GAPDH* and presented as relative expression to that of cells cultured in the absence of rAIM or C75. Error bar indicates SEM.

### FAS as a Target Molecule of Incorporated AIM in Adipocytes

It is of interest that a functional target of AIM is FAS. Through association with multiple regions of FAS (Figure 6C), AIM appears to decrease FAS activity functionally and structurally. The effect of FAS inhibition on the hypothalamus, which influences the fat mass in the body, has been studied extensively. Evidence indicates that systemic administration of C75 decreases the production of neuropeptide Y (NP-Y) in the hypothalamus in mice, resulting in a marked loss of appetite and overall decreased body weight (Loftus et al., 2000; Makimura et al., 2001; Kumar et al., 2002; Mobbs and Makimura, 2002; Shimokawa et al., 2002; Kovacs et al., 2004; Liu et al., 2004; Ronnett et al., 2005; Chakravarthy et al., 2009a). However, $AIM^{-/-}$ and $AIM^{+/+}$ mice showed comparable levels of food intake (Figure S5), suggesting that AIM may not have a neurologic effect. This may be due to the requirement of a specific endocytotic process mediated by CD36, the expression of which is not reported in hypothalamic cells.

Instead, our present results indicate a direct effect of FAS inhibition on adipocytes (brought about by either AIM or C75), which decreases the size and number of lipid droplets, thereby decreasing adipocyte size. There are several possibilities for the mechanism of FAS inhibition in the lipolytic response. Because the inhibition of FAS did not stimulate the cAMP/PKA signaling cascade (Figure S8), it might activate an unknown cAMP/PKA-independent lipolytic pathway. Alternatively, because differentiating adipocytes or mice on a HFD undergo progressive lipogenesis (increase in lipid droplet storage) and constitutive (basal) lipolysis at a substantial level (Holm, 2003; Zechner et al., 2005; Duncan et al., 2007; Lafontan, 2008), the lipolytic outcome on FAS inhibition might simply represent an acute disturbance of lipogenesis. Indeed, it is well known that de novo synthesis of fatty acids via FAS is indispensable for efficient lipogenesis

in bold. A monomer FAS molecule is indicated by a shadowed square. KS, ketoacyl synthase; MAT, malonyl/acetyl transferase; DH, dehydrase; CC, central core; ER, enoylreductase; KR, ketoreductase; ACP, acyl carrier protein; TE, thioesterase.

(D) Dimerized FAS is decreased in the presence of AIM. Cell lysates from 3T3-L1 adipocytes maintained with or without rAIM (5 μg/ml) for 2 days were run on a Tris-acetate gel, and immunoblotting was carried out to assess dimerized (524 kDa) and monomeric (262 kDa) FAS. Sodium dodecyl sulfate (SDS) was removed from the loading buffer to limit potential degradation of the dimerized form.

(E–G) FAS activity in 3T3-L1 adipocytes treated with or without rAIM (5 μg/ml) or C75 (25 μM) for 6 days (E), epididymal fat tissues from $AIM^{+/+}$ and $AIM^{-/-}$ mice (F), and $AIM^{-/-}$ epididymal fat tissue challenged with a local intrafat injection of rAIM or BSA (total 100 μg for each at several loci within the tissue) 3 hr before analysis (G). All mice were fed with a HFD for 20 weeks. Samples were lysed and analyzed for FAS activity. Data are presented for normalized FAS protein levels as assessed by WB using the same samples (data not shown). n = 6 for each group. Error bar indicates SEM.

(Lafontan, 2008). Further discussion related to this issue appears in the Supplemental Information online.

### Same Mechanism for Different Functions?

Whether other functions of AIM, in particular its antiapoptotic effect, are carried out by the same molecular mechanism as that in adipocytes will need to be addressed. As shown in Figure 2B, macrophages also incorporate exogenous AIM, suggesting that AIM functions in macrophages in a manner similar to that in adipocytes. Intriguingly, although AIM inhibits apoptosis in macrophages (Miyazaki et al., 1999; Arai et al., 2005), evidence has shown that suppression of FAS promoted apoptosis in some cancer cells (Lupu and Menendez, 2006; Menendez and Lupu, 2007). However, whether apoptosis is inhibited or accelerated by the suppression of FAS might be dependent on cell type. Certainly, in some cell types, the overexpression of FAS accelerated apoptosis, upregulating the expression of proapoptotic genes (J.K. and T.M., unpublished data). Alternatively, intracellular target molecules of AIM may vary in different cell types and/or in different situations. The mediators for AIM internalization might also vary, given that thymocytes and NK-T cells, in which AIM is also effective (Miyazaki et al., 1999; Kuwata et al., 2003), do not express CD36. This may explain the multiple functions observed for AIM in many cell types.

### Perspectives

In conclusion, we have identified a function of AIM, along with its molecular mechanism, with respect to adipocyte status in fat tissue. The effects of AIM on other organs important for metabolism, such as liver and muscle, remain to be determined. Further investigation will provide new insights into the role of AIM in the pathogenesis of obesity as well as metabolic diseases.

## EXPERIMENTAL PROCEDURES

### Mice

*AIM*$^{-/-}$ mice (Miyazaki et al., 1999) had been backcrossed to C57BL/6 (B6) for 13 generations before being used for experiments. *CD36*$^{-/-}$ mice (Febbraio et al., 1999) were created and maintained by Febbraio in the Lerner Research Institute, Cleveland Clinic Foundation. All mice were maintained under a specific pathogen-free (SPF) condition.

### Statistical Analysis

A two-tailed Mann-Whitney test was used to calculate p values. ***$p < 0.001$, **$p < 0.01$, *$p < 0.05$. Error bars indicate SEM.

Detailed description about reagents for histological analysis, purification of rAIM, in vitro adipogenesis, FAS constructs, efflux analysis of glycerol and FFAs, silver-intensified immunogold for electron microscopy, FAS activity assay, analysis of metabolic rates, quantitative PCR assay, and primers used for experiments appears in the Supplemental Information online.

## SUPPLEMENTAL INFORMATION

Supplemental Information includes Supplemental Discussion, Supplemental Experimental Procedures, Supplemental References, and eight figures and can be found with this article online at doi:10.1016/j.cmet.2010.04.013.

## ACKNOWLEDGMENTS

We thank O. Ohara (Chiba), T. Fujita (Niigata), and T. Ide (Saitama) for useful advice; K. Ikeda and R. Taguchi (Tokyo) as well as Genostaff, Inc. for technical assistance in histology; and M. Egami and M. Miyamoto for preparing the manuscript. This work was supported by Grants-in-Aid for Scientific Research, the Global COE Research Program, Takeda Science Foundation, Research Fund of Mitsukoshi Health and Welfare Foundation, Sankyo Foundation of Life Science, Mitsubishi Pharma Research Foundation, The Mochida Memorial Foundation for Medical and Pharmaceutical Research, Uehara Memorial Foundation, Suzuken Memorial Foundation (to T.M.), Kanae Foundation for the Promotion of Medical Science, Astellas Foundation for Research on Metabolic Disorders, and Ono Medical Research Foundation (to S.A.).

Received: September 14, 2009
Revised: December 18, 2009
Accepted: April 19, 2010
Published: June 8, 2010

## REFERENCES

Ackerman, A.L., Kyritsis, C., Tampé, R., and Cresswell, P. (2005). Access of soluble antigens to the endoplasmic reticulum can explain cross-presentation by dendritic cells. Nat. Immunol. *6*, 107–113.

Apovian, C.M., Bigornia, S., Mott, M., Meyers, M.R., Ulloor, J., Gagua, M., McDonnell, M., Hess, D., Joseph, L., and Gokce, N. (2008). Adipose macrophage infiltration is associated with insulin resistance and vascular endothelial dysfunction in obese subjects. Arterioscler. Thromb. Vasc. Biol. *28*, 1654–1659.

Arai, S., Shelton, J.M., Chen, M., Bradley, M.N., Castrillo, A., Bookout, A.L., Mak, P.A., Edwards, P.A., Mangelsdorf, D.J., Tontonoz, P., and Miyazaki, T. (2005). A role for the apoptosis inhibitory factor AIM/Spalpha/Api6 in atherosclerosis development. Cell Metab. *1*, 201–213.

Asturias, F.J., Chadick, J.Z., Cheung, I.K., Stark, H., Witkowski, A., Joshi, A.K., and Smith, S. (2005). Structure and molecular organization of mammalian fatty acid synthase. Nat. Struct. Mol. Biol. *12*, 225–232.

Baker, J.L., Olsen, L.W., and Sørensen, T.I. (2007). Childhood body-mass index and the risk of coronary heart disease in adulthood. N. Engl. J. Med. *357*, 2329–2337.

Brake, D.K., Smith, E.O., Mersmann, H., Smith, C.W., and Robker, R.L. (2006). ICAM-1 expression in adipose tissue: effects of diet-induced obesity in mice. Am. J. Physiol. Cell Physiol. *291*, C1232–C1239.

Chakravarthy, M.V., Zhu, Y., Yin, L., Coleman, T., Pappan, K.L., Marshall, C.A., McDaniel, M.L., and Semenkovich, C.F. (2009a). Inactivation of hypothalamic FAS protects mice from diet-induced obesity and inflammation. J. Lipid Res. *50*, 630–640.

Chirala, S.S., Chang, H., Matzuk, M., Abu-Elheiga, L., Mao, J., Mahon, K., Finegold, M., and Wakil, S.J. (2003). Fatty acid synthesis is essential in embryonic development: fatty acid synthase null mutants and most of the heterozygotes die in utero. Proc. Natl. Acad. Sci. USA *100*, 6358–6363.

Cinti, S., Mitchell, G., Barbatelli, G., Murano, I., Ceresi, E., Faloia, E., Wang, S., Fortier, M., Greenberg, A.S., and Obin, M.S. (2005). Adipocyte death defines macrophage localization and function in adipose tissue of obese mice and humans. J. Lipid Res. *46*, 2347–2355.

Ducharme, N.A., and Bickel, P.E. (2008). Lipid droplets in lipogenesis and lipolysis. Endocrinology *149*, 942–949.

Duncan, R.E., Ahmadian, M., Jaworski, K., Sarkadi-Nagy, E., and Sul, H.S. (2007). Regulation of lipolysis in adipocytes. Annu. Rev. Nutr. *27*, 79–101.

Farmer, S.R. (2006). Transcriptional control of adipocyte formation. Cell Metab. *4*, 263–273.

Febbraio, M., Abumrad, N.A., Hajjar, D.P., Sharma, K., Cheng, W., Pearce, S.F., and Silverstein, R.L. (1999). A null mutation in murine CD36 reveals an important role in fatty acid and lipoprotein metabolism. J. Biol. Chem. *274*, 19055–19062.

Finn, P.F., and Dice, J.F. (2006). Proteolytic and lipolytic responses to starvation. Nutrition *22*, 830–844.

Gangadharan, B., Antrobus, R., Dwek, R.A., and Zitzmann, N. (2007). Novel serum biomarker candidates for liver fibrosis in hepatitis C patients. Clin. Chem. *53*, 1792–1799.

Gebe, J.A., Kiener, P.A., Ring, H.Z., Li, X., Francke, U., and Aruffo, A. (1997). Molecular cloning, mapping to human chromosome 1 q21-q23, and cell binding characteristics of Spalpha, a new member of the scavenger receptor cysteine-rich (SRCR) family of proteins. J. Biol. Chem. *272*, 6151–6158.

Gebe, J.A., Llewellyn, M., Hoggatt, H., and Aruffo, A. (2000). Molecular cloning, genomic organization and cell-binding characteristics of mouse Spalpha. Immunology *99*, 78–86.

Giodini, A., and Cresswell, P. (2008). Hsp90-mediated cytosolic refolding of exogenous proteins internalized by dendritic cells. EMBO J. *27*, 201–211.

Gray, J., Chattopadhyay, D., Beale, G.S., Patman, G.L., Miele, L., King, B.P., Stewart, S., Hudson, M., Day, C.P., Manas, D.M., and Reeves, H.L. (2009). A proteomic strategy to identify novel serum biomarkers for liver cirrhosis and hepatocellular cancer in individuals with fatty liver disease. BMC Cancer *9*, 271.

Greenwalt, D.E., Lipsky, R.H., Ockenhouse, C.F., Ikeda, H., Tandon, N.N., and Jamieson, G.A. (1992). Membrane glycoprotein CD36: a review of its roles in adherence, signal transduction, and transfusion medicine. Blood *80*, 1105–1115.

Haug, G., Leemhuis, J., Tiemann, D., Meyer, D.K., Aktories, K., and Barth, H. (2003). The host cell chaperone Hsp90 is essential for translocation of the binary Clostridium botulinum C2 toxin into the cytosol. J. Biol. Chem. *278*, 32266–32274.

He, W., Barak, Y., Hevener, A., Olson, P., Liao, D., Le, J., Nelson, M., Ong, E., Olefsky, J.M., and Evans, R.M. (2003). Adipose-specific peroxisome proliferator-activated receptor gamma knockout causes insulin resistance in fat and liver but not in muscle. Proc. Natl. Acad. Sci. USA *100*, 15712–15717.

Holm, C. (2003). Molecular mechanisms regulating hormone-sensitive lipase and lipolysis. Biochem. Soc. Trans. *31*, 1120–1124.

Ibrahimi, A., and Abumrad, N.A. (2002). Role of CD36 in membrane transport of long-chain fatty acids. Curr. Opin. Clin. Nutr. Metab. Care *5*, 139–145.

Joseph, S.B., Bradley, M.N., Castrillo, A., Bruhn, K.W., Mak, P.A., Pei, L., Hogenesch, J., O'connell, R.M., Cheng, G., Saez, E., et al. (2004). LXR-dependent gene expression is important for macrophage survival and the innate immune response. Cell *119*, 299–309.

Kelley, D.S., Nelson, G.J., and Hunt, J.E. (1986). Effect of prior nutritional status on the activity of lipogenic enzymes in primary monolayer cultures of rat hepatocytes. Biochem. J. *235*, 87–90.

Kim, W.K., Hwang, H.R., Kim, H., Lee, P.Y., In, Y.J., Ryu, H.Y., Park, S.G., Bae, K.H., and Lee, S.C. (2008). Glycoproteomic analysis of plasma from patients with atopic dermatitis: CD5L and ApoE as potential biomarkers. Exp. Mol. Med. *40*, 677–685.

Kovacs, P., Harper, I., Hanson, R.L., Infante, A.M., Bogardus, C., Tataranni, P.A., and Baier, L.J. (2004). A novel missense substitution (Val1483Ile) in the fatty acid synthase gene (FAS) is associated with percentage of body fat and substrate oxidation rates in nondiabetic Pima Indians. Diabetes *53*, 1915–1919.

Kuhajda, F.P., Pizer, E.S., Li, J.N., Mani, N.S., Frehywot, G.L., and Townsend, C.A. (2000). Synthesis and antitumor activity of an inhibitor of fatty acid synthase. Proc. Natl. Acad. Sci. USA *97*, 3450–3454.

Kumar, M.V., Shimokawa, T., Nagy, T.R., and Lane, M.D. (2002). Differential effects of a centrally acting fatty acid synthase inhibitor in lean and obese mice. Proc. Natl. Acad. Sci. USA *99*, 1921–1925.

Kuwata, K., Watanabe, H., Jiang, S.Y., Yamamoto, T., Tomiyama-Miyaji, C., Abo, T., Miyazaki, T., and Naito, M. (2003). AIM inhibits apoptosis of T cells and NKT cells in Corynebacterium-induced granuloma formation in mice. Am. J. Pathol. *162*, 837–847.

Lafontan, M. (2008). Advances in adipose tissue metabolism. Int. J Obes. (Lond) *32* (*Suppl 7*), S39–S51.

Lin, S.Y., Makino, K., Xia, W., Matin, A., Wen, Y., Kwong, K.Y., Bourguignon, L., and Hung, M.C. (2001). Nuclear localization of EGF receptor and its potential new role as a transcription factor. Nat. Cell Biol. *3*, 802–808.

Liu, L.H., Wang, X.K., Hu, Y.D., Kang, J.L., Wang, L.L., and Li, S. (2004). Effects of a fatty acid synthase inhibitor on adipocyte differentiation of mouse 3T3-L1 cells. Acta Pharmacol. Sin. *25*, 1052–1057.

Loftus, T.M., Jaworsky, D.E., Frehywot, G.L., Townsend, C.A., Ronnett, G.V., Lane, M.D., and Kuhajda, F.P. (2000). Reduced food intake and body weight in mice treated with fatty acid synthase inhibitors. Science *288*, 2379–2381.

Lupu, R., and Menendez, J.A. (2006). Pharmacological inhibitors of Fatty Acid Synthase (FASN)—catalyzed endogenous fatty acid biogenesis: a new family of anti-cancer agents? Curr. Pharm. Biotechnol. *7*, 483–493.

Madsen, L., Petersen, R.K., Sørensen, M.B., Jørgensen, C., Hallenborg, P., Pridal, L., Fleckner, J., Amri, E.Z., Krieg, P., Furstenberger, G., et al. (2003). Adipocyte differentiation of 3T3-L1 preadipocytes is dependent on lipoxygenase activity during the initial stages of the differentiation process. Biochem. J. *375*, 539–549.

Makimura, H., Mizuno, T.M., Yang, X.J., Silverstein, J., Beasley, J., and Mobbs, C.V. (2001). Cerulenin mimics effects of leptin on metabolic rate, food intake, and body weight independent of the melanocortin system, but unlike leptin, cerulenin fails to block neuroendocrine effects of fasting. Diabetes *50*, 733–739.

Menendez, J.A., and Lupu, R. (2007). Fatty acid synthase and the lipogenic phenotype in cancer pathogenesis. Nat. Rev. Cancer *7*, 763–777.

Miyazaki, T., Hirokami, Y., Matsuhashi, N., Takatsuka, H., and Naito, M. (1999). Increased susceptibility of thymocytes to apoptosis in mice lacking AIM, a novel murine macrophage-derived soluble factor belonging to the scavenger receptor cysteine-rich domain superfamily. J. Exp. Med. *189*, 413–422.

Mobbs, C.V., and Makimura, H. (2002). Block the FAS, lose the fat. Nat. Med. *8*, 335–336.

Neels, J.G., and Olefsky, J.M. (2006). Inflamed fat: what starts the fire? J. Clin. Invest. *116*, 33–35.

Nishino, N., Tamori, Y., Tateya, S., Kawaguchi, T., Shibakusa, T., Mizunoya, W., Inoue, K., Kitazawa, R., Kitazawa, S., Matsuki, Y., et al. (2008). FSP27 contributes to efficient energy storage in murine white adipocytes by promoting the formation of unilocular lipid droplets. J. Clin. Invest. *118*, 2808–2821.

Olshansky, S.J., Passaro, D.J., Hershow, R.C., Layden, J., Carnes, B.A., Brody, J., Hayflick, L., Butler, R.N., Allison, D.B., and Ludwig, D.S. (2005). A potential decline in life expectancy in the United States in the 21st century. N. Engl. J. Med. *352*, 1138–1145.

Olsnes, S., Klingenberg, O., and Wiedłocha, A. (2003). Transport of exogenous growth factors and cytokines to the cytosol and to the nucleus. Physiol. Rev. *83*, 163–182.

Puri, V., and Czech, M.P. (2008). Lipid droplets: FSP27 knockout enhances their sizzle. J. Clin. Invest. *118*, 2693–2696.

Qu, P., Du, H., Li, Y., and Yan, C. (2009). Myeloid-specific expression of Api6/AIM/Sp alpha induces systemic inflammation and adenocarcinoma in the lung. J. Immunol. *182*, 1648–1659.

Ratts, R., Zeng, H., Berg, E.A., Blue, C., McComb, M.E., Costello, C.E., vanderSpek, J.C., and Murphy, J.R. (2003). The cytosolic entry of diphtheria toxin catalytic domain requires a host cell cytosolic translocation factor complex. J. Cell Biol. *160*, 1139–1150.

Ronnett, G.V., Kim, E.K., Landree, L.E., and Tu, Y. (2005). Fatty acid metabolism as a target for obesity treatment. Physiol. Behav. *85*, 25–35.

Rosen, E.D., Sarraf, P., Troy, A.E., Bradwin, G., Moore, K., Milstone, D.S., Spiegelman, B.M., and Mortensen, R.M. (1999). PPAR gamma is required for the differentiation of adipose tissue in vivo and in vitro. Mol. Cell *4*, 611–617.

Sandvig, K., and van Deurs, B. (2000). Entry of ricin and Shiga toxin into cells: molecular mechanisms and medical perspectives. EMBO J. *19*, 5943–5950.

Sandvig, K., and van Deurs, B. (2005). Delivery into cells: lessons learned from plant and bacterial toxins. Gene Ther. *12*, 865–872.

Schmid, B., Rippmann, J.F., Tadayyon, M., and Hamilton, B.S. (2005). Inhibition of fatty acid synthase prevents preadipocyte differentiation. Biochem. Biophys. Res. Commun. *328*, 1073–1082.

Shimokawa, T., Kumar, M.V., and Lane, M.D. (2002). Effect of a fatty acid synthase inhibitor on food intake and expression of hypothalamic neuropeptides. Proc. Natl. Acad. Sci. USA *99*, 66–71.

Shoelson, S.E., Lee, J., and Goldfine, A.B. (2006). Inflammation and insulin resistance. J. Clin. Invest. *116*, 1793–1801.

Smas, C.M., and Sul, H.S. (1993). Pref-1, a protein containing EGF-like repeats, inhibits adipocyte differentiation. Cell *73*, 725–734.

Smith, S. (1994). The animal fatty acid synthase: one gene, one polypeptide, seven enzymes. FASEB J. *8*, 1248–1259.

Smith, S., Stern, A., Randhawa, Z.I., and Knudsen, J. (1985). Mammalian fatty acid synthetase is a structurally and functionally symmetrical dimer. Eur. J. Biochem. *152*, 547–555.

Surmi, B.K., and Hasty, A.H. (2008). Macrophage infiltration into adipose tissue: initiation, propagation and remodeling. Future Lipidol. *3*, 545–556.

Valledor, A.F., Hsu, L.C., Ogawa, S., Sawka-Verhelle, D., Karin, M., and Glass, C.K. (2004). Activation of liver X receptors and retinoid X receptors prevents bacterial-induced macrophage apoptosis. Proc. Natl. Acad. Sci. USA *101*, 17813–17818.

Wesche, J., Małecki, J., Wiedłocha, A., Skjerpen, C.S., Claus, P., and Olsnes, S. (2006). FGF-1 and FGF-2 require the cytosolic chaperone Hsp90 for translocation into the cytosol and the cell nucleus. J. Biol. Chem. *281*, 11405–11412.

Wu, Z., Puigserver, P., and Spiegelman, B.M. (1999a). Transcriptional activation of adipogenesis. Curr. Opin. Cell Biol. *11*, 689–694.

Wu, Z., Rosen, E.D., Brun, R., Hauser, S., Adelmant, G., Troy, A.E., McKeon, C., Darlington, G.J., and Spiegelman, B.M. (1999b). Cross-regulation of C/EBP alpha and PPAR gamma controls the transcriptional pathway of adipogenesis and insulin sensitivity. Mol. Cell *3*, 151–158.

Yusa, S., Ohnishi, S., Onodera, T., and Miyazaki, T. (1999). AIM, a murine apoptosis inhibitory factor, induces strong and sustained growth inhibition of B lymphocytes in combination with TGF-β1. Eur. J. Immunol. *29*, 1086–1093.

Zechner, R., Strauss, J.G., Haemmerle, G., Lass, A., and Zimmermann, R. (2005). Lipolysis: pathway under construction. Curr. Opin. Lipidol. *16*, 333–340.

Cell Metabolism
Article

# A Liver-Derived Secretory Protein, Selenoprotein P, Causes Insulin Resistance

Hirofumi Misu,[1,10] Toshinari Takamura,[1,10,*] Hiroaki Takayama,[1] Hiroto Hayashi,[1] Naoto Matsuzawa-Nagata,[1] Seiichiro Kurita,[1] Kazuhide Ishikura,[1] Hitoshi Ando,[1] Yumie Takeshita,[1] Tsuguhito Ota,[1] Masaru Sakurai,[1] Tatsuya Yamashita,[1] Eishiro Mizukoshi,[1] Taro Yamashita,[1] Masao Honda,[1] Ken-ichi Miyamoto,[2,3] Tetsuya Kubota,[4] Naoto Kubota,[4] Takashi Kadowaki,[4] Han-Jong Kim,[5] In-kyu Lee,[5] Yasuhiko Minokoshi,[6] Yoshiro Saito,[7] Kazuhiko Takahashi,[8] Yoshihiro Yamada,[9] Nobuyuki Takakura,[9] and Shuichi Kaneko[1]

[1]Department of Disease Control and Homeostasis
[2]Department of Hospital Pharmacy
[3]Department of Medicinal Informatics
Kanazawa University Graduate School of Medical Science, Kanazawa, Ishikawa 920-8641, Japan
[4]Department of Diabetes and Metabolic Diseases, Graduate School of Medicine, University of Tokyo, Tokyo 113-8655, Japan
[5]Section of Endocrinology, Department of Internal Medicine, Kyungpook National University Hospital, School of Medicine, Kyungpook National University, Jungu, Daegu 700-412, Korea
[6]Division of Endocrinology and Metabolism, Department of Developmental Physiology, National Institute for Physiological Sciences, Okazaki, Aichi 444-8585, Japan
[7]Department of Medical Life Systems, Faculty of Medical and Life Sciences, Doshisha University, Kyotanabe, Kyoto 610-0394, Japan
[8]Department of Nutritional Biochemistry, Hokkaido Pharmaceutical University, Otaru, Hokkaido 047-0264, Japan
[9]Department of Signal Transduction, Research Institute for Microbial Diseases, Osaka University, Osaka 565-0871, Japan
[10]These authors contributed equally to this work
*Correspondence: ttakamura@m-kanazawa.jp
DOI 10.1016/j.cmet.2010.09.015

## SUMMARY

**The liver may regulate glucose homeostasis by modulating the sensitivity/resistance of peripheral tissues to insulin, by way of the production of secretory proteins, termed hepatokines. Here, we demonstrate that selenoprotein P (SeP), a liver-derived secretory protein, causes insulin resistance. Using serial analysis of gene expression (SAGE) and DNA chip methods, we found that hepatic SeP mRNA levels correlated with insulin resistance in humans. Administration of purified SeP impaired insulin signaling and dysregulated glucose metabolism in both hepatocytes and myocytes. Conversely, both genetic deletion and RNA interference-mediated knockdown of SeP improved systemic insulin sensitivity and glucose tolerance in mice. The metabolic actions of SeP were mediated, at least partly, by inactivation of adenosine monophosphate-activated protein kinase (AMPK). In summary, these results demonstrate a role of SeP in the regulation of glucose metabolism and insulin sensitivity and suggest that SeP may be a therapeutic target for type 2 diabetes.**

## INTRODUCTION

Insulin resistance is an underlying feature of people with type 2 diabetes and metabolic syndrome (Saltiel and Kahn, 2001), but is also associated with risk for cardiovascular diseases (Després et al., 1996) and contributes to the clinical manifestations of nonalcoholic steatohepatitis (Ota et al., 2007). In an insulin-resistant state, impaired insulin action promotes hepatic glucose production and reduces glucose uptake by peripheral tissues, resulting in hyperglycemia. The molecular mechanisms underlying insulin resistance are not fully understood, but are now known to be influenced by the secretion of tissue-derived factors, traditionally considered separate from the endocrine system. Recent work in obesity research, for example, has demonstrated that adipose tissues secrete a variety of proteins, known as adipocytokines (Friedman and Halaas, 1998; Maeda et al., 1996; Scherer et al., 1995; Steppan et al., 2001; Yang et al., 2005), which can either enhance or impair insulin sensitivity, thereby contributing to the development of insulin resistance.

SeP (in humans encoded by the *SEPP1* gene) is a secretory protein primarily produced by the liver (Burk and Hill, 2005; Carlson et al., 2004). It contains ten selenocysteine residues and functions as a selenium supply protein (Saito and Takahashi, 2002). However, the role of SeP in the regulation of glucose metabolism and insulin sensitivity has not yet been established. Furthermore, the clinical significance of SeP in human diseases has not been well defined, although studies of SeP knockout mice showed SeP deficiency to be associated with neurological injury and low fertility (Hill et al., 2003; Schomburg et al., 2003).

The liver plays a central role in glucose homeostasis and is also the site for the production of various secretory proteins. For example, recent work in our laboratory has revealed that genes encoding secretory proteins are abundantly expressed in the livers of people with type 2 diabetes (Misu et al., 2007). Moreover, genes encoding angiogenic factors, fibrogenic factors, and redox-associated factors were differentially expressed in the livers of people with type 2 diabetes (Takamura et al., 2004; Takeshita et al., 2006), possibly contributing to the pathophysiology of

type 2 diabetes and its clinical manifestations. On the basis of these findings, we hypothesize that, analogous to adipose tissues, the liver may also contribute to the development of type 2 diabetes and insulin resistance, through the production of secretory proteins, termed hepatokines.

## RESULTS

### Identification of a Hepatic Secretory Protein Involved in Insulin Resistance

To identify hepatic secretory proteins involved in insulin resistance, we performed liver biopsies in humans and conducted a comprehensive analysis of gene expression profiles, using two distinct methods. First, we obtained human liver samples from five patients with type 2 diabetes and five nondiabetic subjects who underwent surgical procedures for malignant tumors, and we subjected them to serial analysis of gene expression (SAGE) (Velculescu et al., 1995). Consequently, we identified 117 genes encoding putative secretory proteins with expression levels in people with type 2 diabetes, 1.5-fold or greater higher than those in normal subjects. Next, we obtained ultrasonography-guided percutaneous needle liver biopsies from ten people with type 2 diabetes and seven normal subjects (Table S1 available online), and we subjected them to DNA chip analysis to identify genes whose hepatic expression was significantly correlated with insulin resistance (Table S2). We performed glucose clamp experiments on these human subjects and measured the metabolic clearance rate (MCR) of glucose (glucose infusion rate divided by the steady-state plasma glucose concentration) as a measure of systemic insulin sensitivity. As a result, we found that *SEPP1* expression levels were upregulated 8-fold in people with type 2 diabetes compared with normal subjects, as determined by SAGE (Table S2). Additionally, there was a negative correlation between hepatic *SEPP1* messenger RNA (mRNA) levels and the MCR of glucose, indicating that elevated hepatic *SEPP1* mRNA levels were associated with insulin resistance (Figure 1A). As a corollary, we found a positive correlation between the levels of hepatic *SEPP1* mRNA and postloaded or fasting plasma glucose (Figures 1B and 1C).

### Elevation of SeP in Type 2 Diabetes

To characterize the role of SeP in the development of insulin resistance, we measured serum SeP levels in human samples (Table S3), using enzyme-linked immunosorbent assays (ELISA), as described previously (Saito et al., 2001). Consistent with elevated hepatic *SEPP1* mRNA levels, we found a significant positive correlation between serum SeP levels and both fasting plasma glucose and hemoglobin $A_{1c}$ ($HbA_{1c}$) levels (Figures 1D and 1E). $HbA_{1c}$ is a clinical marker of protein glycation due to hyperglycemia, and elevated $HbA_{1c}$ levels generally reflect poor glucose control over a 2–3 month period. Additionally, serum levels of SeP were significantly elevated in people with type 2 diabetes compared with normal subjects (Figure 1F and Table S4). Similar to data derived from clinical specimens, in rodent models of type 2 diabetes, including OLETF rats and KKAy mice, hepatic *Sepp1* mRNA and serum SeP levels were elevated (Figures 1G–1J and Table S5).

### SeP Expression in Hepatocytes Is Regulated by Glucose, Palmitate, and Insulin

To clarify the pathophysiology contributing to the hepatic expression of SeP in type 2 diabetes, we investigated the effects of nutrient supply on *Sepp1* mRNA expression in cultured hepatocytes. We found that the addition of glucose or palmitate upregulated *Sepp1* expression, whereas insulin downregulated it in a dose- and time-dependent manner (Figures 2A, 2C, 2E, and 2F). Similar effects on SeP protein levels were observed in primary mouse hepatocytes (Figures 2B, 2D, and 2G). Consistent with the negative regulation of *Sepp1* by insulin in hepatocytes, *Sepp1* mRNA levels were elevated in the livers of fasting C57BL6J mice, compared with those that had been fed (Figure 2H). Thus, multiple lines of evidence suggest that elevated SeP is associated with the development of insulin resistance.

### SeP Impairs Insulin Signaling and Dysregulates Glucose Metabolism In Vitro

Because there is no existing cell culture or animal model in which SeP is overexpressed, we purified SeP from human plasma using chromatographic methods (Saito et al., 1999; Saito and Takahashi, 2002) to examine the effects of SeP on insulin-mediated signal transduction. Treatment of primary hepatocytes with purified SeP induced a reduction in insulin-stimulated phosphorylation of insulin receptor (IR), and Akt (Figures 3A and 3B). SeP exerts its actions through an increase in cellular glutathione peroxidase (Saito and Takahashi, 2002). Coadministration of BSO, a glutathione synthesis inhibitor, rescued cells from the inhibitory effects of SeP (Figure 3C). Moreover, SeP increased phosphorylation of IRS1 at Ser307, the downregulator of tyrosine phosphorylation of IRS (Figure S1A). Similar effects of SeP were also observed in C2C12 myocytes (Figure S1B). Next, we assessed whether SeP dysregulated cellular glucose metabolism. In H4IIHEC hepatocytes, treatment with SeP upregulated mRNA expression of *Pck1* and *G6pc*, key gluconeogenic enzymes, resulting in a 30% increase in glucose release in the presence of insulin (Figures 3D–3F). Treatment with SeP alone had no effects on the levels of mRNAs encoding gluconeogenic enzymes or on glucose production in the absence of insulin, suggesting that SeP modulates insulin signaling. Additionally, treatment with SeP induced a reduction in insulin-stimulated glucose uptake in C2C12 myocytes (Figure 3G). These in vitro experiments indicate that, at physiological concentrations, SeP impairs insulin signal transduction and dysregulated cellular glucose metabolism.

### SeP Impairs Insulin Signaling and Disrupts Glucose Homeostasis In Vivo

To examine the physiological effects of SeP in vivo, we treated female C57BL/6J mice with two intraperitoneal injections of purified human SeP (1 mg/kg body weight), 12 and 2 hr before the experiments. Injection of purified human SeP protein resulted in serum levels of 0.5–1.5 μg/mL (data not shown). These levels correspond to the incremental change of SeP serum levels in people with normal glucose tolerance to those with type 2 diabetes (Saito et al., 2001). Glucose and insulin tolerance tests revealed that treatment of mice with purified SeP induced glucose intolerance and insulin resistance (Figures 3H and 3I). Blood insulin levels were significantly elevated in

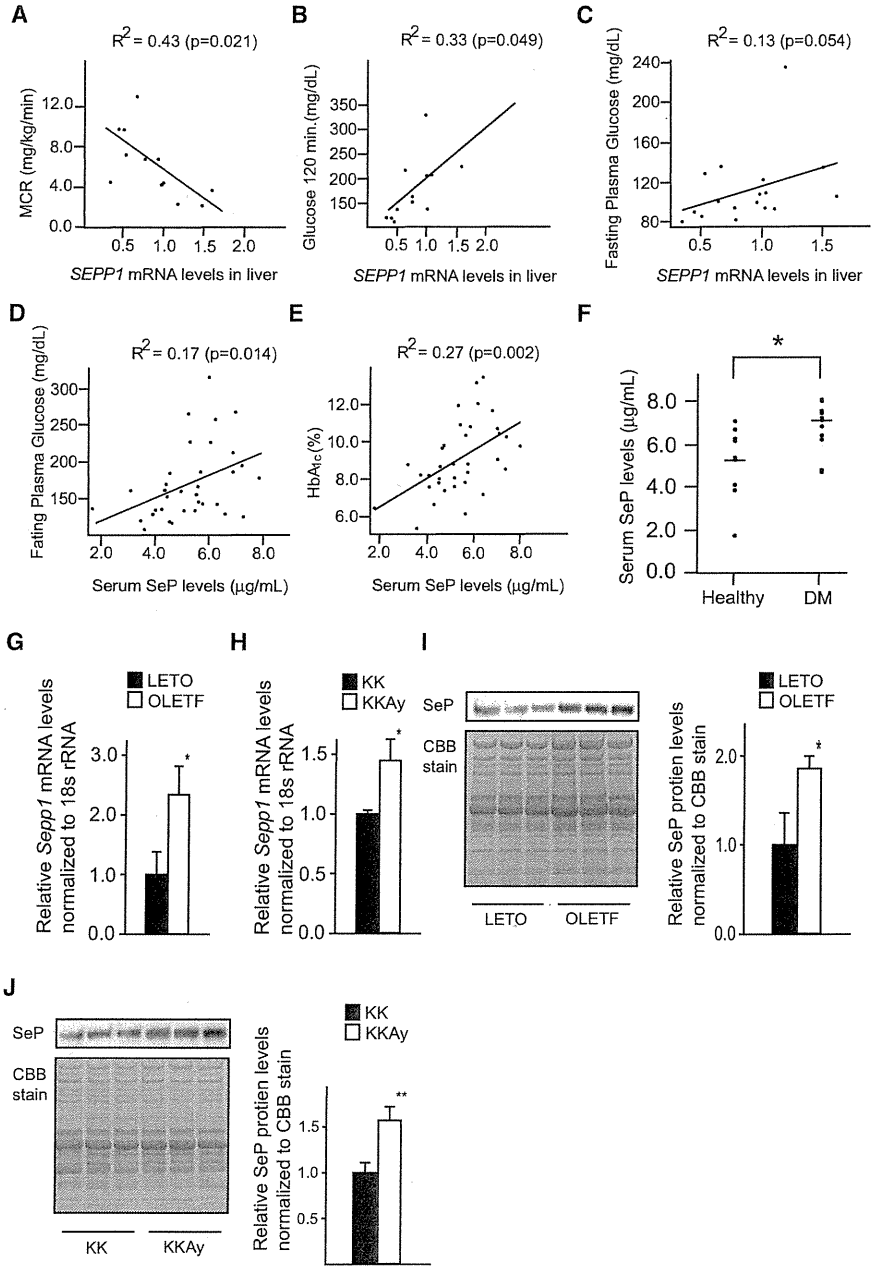


**Figure 1. Elevation of Serum SeP Levels and Hepatic *Sepp1* Expression in Type 2 Diabetes**

(A–C) Individual correlations between hepatic *SEPP1* mRNA levels and metabolic clearance rate (MCR) of glucose (A), postloaded plasma glucose levels (B), and fasting plasma glucose levels (C) in humans (n = 12–17). MCR equals the glucose infusion rate divided by the steady-state plasma glucose concentration, and is a measure of systemic insulin sensitivity. MCR values were determined by glucose clamp. *SEPP1* mRNA levels were quantified with DNA chips.

(D and E) Correlations between serum levels of SeP and fasting plasma glucose levels (D) and $HbA_{1c}$ (E) in people with type 2 diabetes (n = 35).

(F) Serum levels of SeP in people with type 2 diabetes and healthy subjects (n = 9–12). Age and body weight were not significantly different between the two groups. Data represents the means ± SEM from two groups. *p < 0.05.

(G and H) Hepatic *Sepp1* mRNA levels in an animal model of type 2 diabetes (n = 5–6).

(I and J) Serum SeP levels in an animal model of type 2 diabetes. SeP was detected by western blotting. Coomassie brilliant blue (CBB)-stained gel is used as a control for protein loading. Graphs display the results of densitometric quantification, normalized to CBB-stained proteins (n = 5).

Data represent the mean ± SEM from five to six mice per group. *p < 0.05, **p < 0.01. See also Tables S1–S5.

SeP-injected mice, although those of glucagon and GLP-1 were unaffected during a glucose tolerance test (Figure S1C). Western blot analysis showed a reduction in insulin-induced serine phosphorylation of Akt in both liver and skeletal muscle of SeP-injected mice (Figures 3J and 3K). Hyperinsulinemic-euglycemic clamp studies showed that treatment with SeP significantly increased endogenous glucose production and decreased peripheral glucose disposal (Figure S1D and Figures 3L and 3M). Additionally, serum levels of injected human SeP protein negatively correlated with rates of peripheral glucose disposal (Figure S1E). These data indicate that SeP impairs insulin signaling in the liver and skeletal muscle and induces glucose intolerance in vivo.

## Knockdown of *Sepp1* in Liver Improves Glucose Intolerance and Insulin Resistance in Mice with Type 2 Diabetes

To determine whether knockdown of endogenous *Sepp1* enhances insulin signaling, we transfected H4IIEC hepatocytes with *Sepp1*-specific small interfering RNA (siRNA), and we observed a reduction in endogenous *Sepp1* mRNA and SeP protein levels (Figures 4A and 4B). Insulin-stimulated serine phosphorylation of Akt was enhanced in these treated cells (Figure 4C). Similarly, delivery of *Sepp1*-specific siRNAs into KKAy mice via a hydrodynamic transfection method (McCaffrey et al., 2002; Zender et al., 2003) resulted in a 30% reduction in SeP protein levels in the liver and blood (Figures 4D–4G and Figure S2). Knockdown of *Sepp1* improved both glucose intolerance (Figures 4H and 4I) and insulin resistance (Figures 4J and 4K) in KKAy mice.

## SeP-Deficient Mice Show Improved Glucose Tolerance and Enhanced Insulin Signaling in Liver and Muscle

We further confirmed the long-term effects of lowered SeP using *Sepp1* knockout mice (Hill et al., 2003). SeP knockout mice were viable and displayed normal body weights when maintained on a selenium-sufficient diet. Body weight, food intake, and $O_2$ consumption were unaffected by SeP knockout (Figures S3A

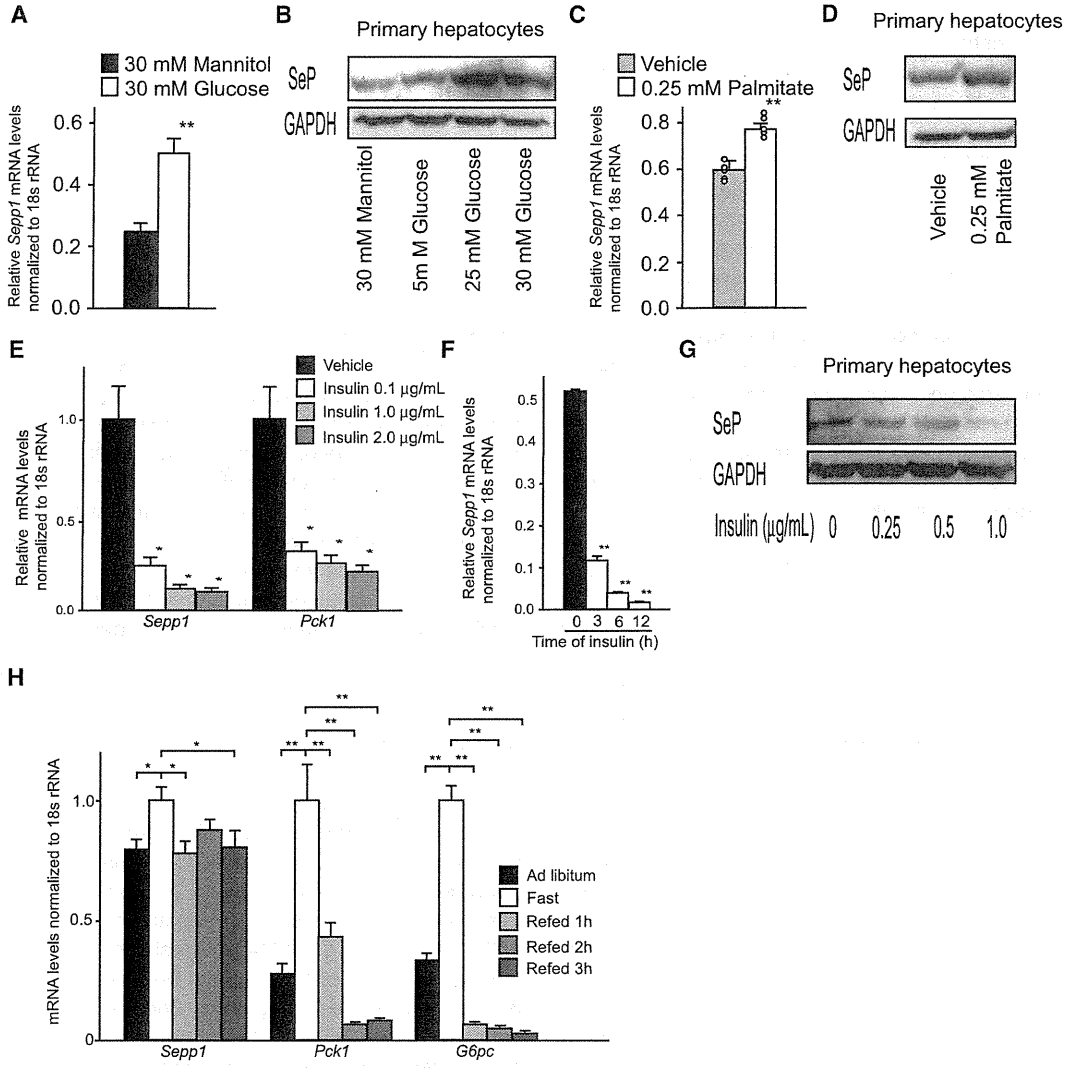


**Figure 2. SeP Expression Is Regulated by Glucose, Palmitate, and Insulin**

(A) *Sepp1* mRNA levels in H4IIEC hepatocytes treated with glucose or mannitol (30 mM) for 6 hr (n = 4).

(B) SeP protein levels in primary hepatocytes treated with glucose or mannitol for 6 hr.

(C) *Sepp1* mRNA levels in H4IIEC hepatocytes treated with palmitate (0.25 mM) for 16 hr (n = 5).

(D) SeP protein levels in primary hepatocytes treated with palmitate (0.25 mM) for 16 hr.

(E) *Sepp1* and *Pck1* mRNA levels in H4IIEC hepatocytes treated with various concentrations of insulin for 6 hr (n = 4).

(F) *Sepp1* mRNA levels in H4IIEC hepatocytes treated with insulin (0.1 μg/ml) for the indicated periods of time (n = 4).

(G) SeP protein levels in primary hepatocytes treated with various concentrations of insulin for 6 hr.

(H) Liver *Sepp1*, *Pck1*, and *G6pc* mRNA levels in C57BL/6J mice following fasting for 12 hr and subsequent refeeding (n = 4).

Data in (A), (C), (E), and (F) represent the means ± SEM from four to five cells per group, and data in (H) represent the means ± SEM from four mice per group. *p < 0.05, **p < 0.01.

and S3B). Lipid accumulation in the liver and adipose tissues was also unaffected (Figure 5A). However, postprandial plasma levels of insulin were reduced in *Sepp1*$^{-/-}$ mice, although blood glucose levels remained unchanged (Figures 5B and 5C). Glucose loading test revealed that *Sepp1*$^{-/-}$ mice showed improved glucose tolerance (Figure 5D). Insulin loading test revealed that *Sepp1*$^{-/-}$ mice showed lower blood glucose levels 60 min after insulin injection (Figure 5E). Insulin signaling, including phosphorylation of Akt and insulin receptor, was enhanced in the liver and skeletal muscle of *Sepp1*$^{-/-}$ mice (Figures 5F–5K). Additionally, *Sepp1*$^{+/-}$ tended to show enhanced insulin sensitivity. Plasma levels of glucagon, active GLP-1, and total GIP were unaffected by the loss of SeP in both fasted and fed mice (Figure S3C), suggesting that SeP dysregulated glucose metabolism in vivo primarily by modulating the insulin pathway, but not by affecting other hormones, including glucagon, GLP-1, and GIP.

### SeP Deficiency Attenuates Adipocyte Hypertrophy and Insulin Resistance in Dietary Obese Mice

To determine whether SeP deficiency reduces insulin resistance caused by diet-induced obesity, we fed SeP knockout mice